THE ROLE OF CELL CYCLE IN DIRECT REPROGRAMMING OF INDUCED CARDIOMYOCYTES

（心筋への直接転換における細胞周期の機能解析）

BY

Emre BEKTIK

Submitted in fulfillment of the requirements
for the degree of Doctor of Philosophy in Human Biology in the Graduate School of Integrative and Global Majors at
UNIVERSITY OF TSUKUBA, 2017

DISSERTATION COMMITTEE:

Prof. Hitoshi SHIMANO, Chair (U. of Tsukuba)

Prof. Satoru TAKAHASHI (U. of Tsukuba)

Prof. Akiyoshi FUKAMIZU (U. of Tsukuba)

Prof. Arthur D. LANDER (U. of California, Irvine)

ACKNOWLEDGEMENT

I owe a great thank to Dr. Jidong FU for his great mentorship as well as a great friendship during my Ph.D. training. This piece of work would not have been possible without his compassion and scientific vision. During my Ph.D. training in his laboratory, I really enjoyed working with him and other members of Heart and Vascular Research Center at Case Western Reserve University.

I would like to specially thank my supervisor Prof. Satoru TAKAHASHI for his generosity to help me all this time. He is a great and smart researcher and a wonderful supervisor for all his students including me. Professor Takahashi, thank you very much to never get angry with me.

Beside my great appreciations to my mentor and supervisor, I also feel very grateful for kind helps and discussions from my co-advisors Professor Arthur D. LANDER (University of California, Irvine) and Prof. Hiromi YANAGISAWA (University of Tsukuba) for my dissertation study.

I also feel very grateful to my committee members, Professors Hitoshi SHIMANO and Akiyoshi FUKAMIZU, for their kindness and generosity to help revising my dissertation presentation and documents.

Finally, I would like to admit that I would not be standing alone all this time by myself without all those supports from my parents and sisters as well as all my friends in Tsukuba (Japan), Tokyo (Japan), and Cleveland (USA). Thank you very much for being so patient so far that I could not have enough time with you, especially with my parents.

THESIS OUTLINE

CHAPTER 1

GENERAL BACKGROUND

1.1. INTRODUCTION

Mortality by CVDs (cardiovascular diseases) accounts for 31% of all deaths worldwide (World Health Organization, 2015). The most common form of heart disease is CAD (coronary artery disease) where functional CMs (cardiomyocytes) die out in the heart and are replaced by fibrotic scar. This eventually causes decreased heart function and heart failure leading to heart attacks or stroke. Since adult CMs possess very limited self-regenerative capability, heart transplantation has been the most effective way of therapy for heart patients. However, limited access to donor organs and existence of potential problems with immunosuppression and graft vascularization, heart transplantation is a limited option for most patients with end-stage heart diseases. Rather, cellular therapies offer a more accessible option for a broader group of coronary heart patients. Currently, there are four major cellular therapy approaches: 1) transplantation of autologous adult stem cells, 2) transplantation of ESC- or iPSC-derived CMs, 3) forced proliferation of adult CMs, and 4) cell fate reprogramming. Transplantation of autologous adult stem cells, such as progenitor cells and bone marrow-derived MSCs, provides very limited regeneration, as they are not differentiating into CMs but rather providing some cardioprotection through paracrine signaling. Another approach is the transplantation of differentiated CMs from pluripotent stem cells. They also possess limited benefit to heart function since in vitro differentiated CMs are immature, show limited coupling with the resident CMs, and possess limited viability. Third approach is the forced cell-cycle reentry of adult CMs. Cell cycle reentry in CMs carry potential concerns regarding efficacy and safety. It is still unknown if proposed methods can provide sufficient number of CMs for a potential clinical therapy. On the other side, non-specific cell cycle activation in the resident non-myocyte cells might induce tumorigenesis. Forth approach is the direct cardiac reprogramming of resident non-myocytes in the scar into functional iCMs (induced cardiomyocytes). In this chapter, I will review the discovery and progress of direct cardiac reprogramming.

1.2. HISTORY AND PROGRESS OF DIRECT CARDIAC REPROGRAMMING

1.2.1. Development of Direct Cardiac Reprogramming by Cardiac Transcription Factors

A single transcription factor, MyoD, has been identified as the master regulator of skeletal muscle cells, yet it has not been known if any master regulator exists for other cell lineages until the discovery of induced pluripotent stem cells (iPSCs) in 2006 [1] A single transcription factor was not enough to induce iPSCs from fibroblasts, however, a combination of *Oct4, Sox2, Klf4, and c-Myc* were able to convert a terminally differentiated cell type into pluripotent cells [2]. Discovery of iPSCs opened a new avenue for direct reprogramming of adult cell types into different cell lineages [3]. In 2010, Ieda et al [4] discovered a minimal combination of transcription factors (GMT: Gata4, Mef2c, and Tbx5), which convert cardiac fibroblasts into induced cardiomyocytes (iCMs). They utilized a cardiac reporter gene expressing GFP under the promoter of aMHC (aMHC-GFP), which was expressed in reprogrammed cells [4]. aMHC-GFP^{+} iCMs expressed a group of cardiac genes, e.g. Mhy6, Actc1, Actn2, etc., and showed sarcomere assembly. 2 weeks after reprogramming induction, some iCMs showed spontaneous calcium oscillations and 0.01-0.1% of transduced cells were able to spontaneously beat. Besides, iCMs had action potentials similar to ventricular cardiomyocytes. Moreover, iCMs did not express progenitor markers, cKit, Isl1 and Mesp1 during reprogramming initiation, suggesting that GMT directly reprogrammed iCMs without an intermediate stem/progenitor cell stage.

Transcription factor-based approach has been used for discovering new methods to improve reprogramming efficiency and quality. Song et al added Hand2 to GMT cocktail (GHMT) and improved in vivo reprogramming efficiency [5]. They had 3-fold more aMHC-GFP/cTnT double-positive iCMs in adult murine tail-tip fibroblasts (TTFs) and 5-fold more in adult cardiac fibroblasts than with GMT. They also showed GHMT could induce beating iCMs, suggesting Hand2 is a reprogramming enhancer. Protze et al [6] screened a library of transcription factors and found that an optimal combination of Mef2c, Tbx5, and Myocd could generate iCMs positive for multiple cardiac

genes. Addis et al [7] used a different reporter system in which the calcium indicator GCaMP is coexpressed with human cTnT. They added Nkx2.5 to GHMT reprogramming factors and showed 50-fold more iCMs with spontaneous calcium oscillations, cardiomyocyte markers, and spontaneous beating. Hirai et al [8] fused MyoD domain to Gata4, Hand2, Mef2c, and Tbx5 and transduced fusion genes into non-cardiac fibroblasts. MyoD-Mef2c fusion with other three wild-type genes yielded 15-fold more beating iCMs than transduction with combination of all 4 wild-type genes.

1.2.2. Generating iCMs without Cardiac Transcription Factors

By a different approach from transcription factor-based system, Jayawardena et al [9] tested a combination of microRNAs (miRs) for their iCM induction ability. A combination of muscle-specific miRs (miR1, miR133, miR208, and miR409) could induce iCMs from mouse CFs. JAK inhibitor improved reprogramming capability of miR combo [9]. Their study did not demonstrate mechanism of reprogramming by miRs and functional aspects of iCMs generated with miRs have not been well studied. Muraoka et al [10] showed that miR133 improved number of beating iCMs 7-fold in MEFs compare to GMT alone and shortened time of beating iCMs after gene transduction through suppression of Snai1, a master regulator of epithelial-to-mesenchymal transition.

Alternatively, Wang et al [11] reported that cardiac reprogramming could be achieved without cardiac transcription factors. They used four compounds (SB431542, CHIR99021, Parnate, and Forskolin) together with Oct4 transduction. Mouse fibroblasts were converted into iCMs by passing through a cardiac precursor state and mostly converted into ventricular cardiomyocyte-like cells. Moreover, Fu et al [12] succeeded to reprogram chemical-induced cardiomyocyte-like cells (CiCMs) from mouse fibroblasts by only a chemical compound cocktail consisted of CHIR99021, RepSox, Forskolin, VPA, Parnate, TTNPB, and DZnep (CRFVPTZ). CiCMs passed through a cardiac progenitor stage by upregulating Sca-1, Wt1, Flk1, Abcg2, and Mesp1 in the early stages of reprogramming, yet also expressed pluripotency markers, Oct4, Nanog, Sox2, Rex1, at low levels. However, CiCMs generated from fibroblasts of Oct4-GFP mice did not induce Oct4-GFP+ cells, suggesting that CiCMs pass

through a cardiac progenitor state, but not a pluripotent stage. Similarly, Cao et al [13] showed that human fibroblasts could also be converted into beating iCMs with a combination of chemical compounds, composed of CHIR99021, A83-01, BIX01294, AS8351, SC1, Y27632, OAC2, SU16F, and JNJ10198409. They also showed that cells were initially passed through a progenitor stage and finally converted into functional iCMs, suggesting that chemical compound-based reprogramming has a different mechanism of reprogramming from cardiac reprogramming with GMT transcription factors.

1.2.3. Attempts to Reveal Mechanism of Cardiac Reprogramming

Activation or inhibition of signaling pathways has been shown to alter efficiency of iCM reprogramming. Ifkovits et al [14] demonstrated that inhibition of transforming growth factor beta (TGF-b) enhanced reprogramming of iCMs in MEFs and CFs. Zhao et al [15] showed that inhibition of Rho-associated kinase (ROCK) pathway increased conversion rate of iCMs in MEFs, TTFs, and CFs. Conversely, activation of TGF-b or ROCK in iCMs attenuated cardiac reprogramming, suggesting that profibrotic signaling is a barrier to reprogramming induction. Our study showed that ~16% of iCMs in early stages of reprogramming was apoptosized (**Unpublished data**), that's why; ROCK inhibitors might improve reprogramming by suppressing apoptosis in reprogrammed iCMs. Zhou et al [16] demonstrated that overexpression of Akt1 together with GHMT transcription factors reprogrammed 50% of MEFs into iCMs with spontaneous beating as early as day 20. Akt1 improved maturation of iCMs through activation of Akt1 downstream targets, mTORC1 and Foxo3a. On the other hand, Yamakawa et al [17] defined a serum-free condition with combination of FGF2, FGF10, and VEGF (FFV), which improved induction of beating iCMs compare to serum-based culture. FFV enhanced reprogramming through activation of endogenous Gata4 and activation of MAP kinase and PI3K/Akt pathways. Additionally, Wnt signaling inhibition by IWP4 further improved induction of beating iCMs with FFV.

We also had an effort to enlighten a part of the mechanism of reprogramming in murine cells. We facilitated cell cycle exit through transient arrest of cell cycle at S or G2/M phase after transduction of GMT single factors. Our data showed that iCMs arrested at S or G2/M diminished proliferation and inhibited cell cycle genes, yet improved cardiac gene expression. Our finding suggested that cell cycle exit is a required process for faster maturation of iCMs (**Unpublished data**). Similarly, a single polycistronic MGT construct, generated by Wang et al [18], facilitated cell cycle exit and improved maturity of iCMs in our hands (**Unpublished data**). MGT offers an optimal stoichiometry of transcription factors compared to mixture of single factors with heterogeneous expression. We demonstrated that MGT stoichiometry offers a better reprogramming by inducing cell cycle exit in an earlier stage than single GMT factors could do.

Reprogramming of iCMs requires overcoming epigenetic barriers that were established in fibroblasts. Modulation of epigenetic states in the cells improves reprogramming success. Liu et al [19] analyzed histone and DNA methylations in iCMs generated by a polycistronic MGT. MGT increased expression of trimethylated histone H3 of lysine 4 (H3K4me3), which marks active chromatin, and diminished trimethylated histone H3 of lysine 27 (H3K27me3), which marks inactive chromatin, in cardiac gene promoters as early as day3 of MGT transduction. On the contrary, MGT decreased H3K4me3 and increased H3K27me3 in fibroblast genes. Moreover, DNA methylations on CpG islands on the promoters of cardiac genes Mhy6 and Nppa were decreased within 3 days of MGT transduction, suggesting DNA methylation on cardiac gene promoters as a barrier for cardiac reprogramming. The study by Zhou et al [20] similarly demonstrated that Bmi1 suppression improved induction of iCMs through decreased methylation on cardiac genes.

1.2.4. Direct Reprogramming of Human Fibroblasts

To be able to translate cardiac reprogramming to clinical therapies, it is essential to optimize reprogramming cocktails for human cells and understand the mechanism of reprogramming. Research teams including ours investigated cardiac reprogramming in human fibroblasts. Nam et al [21]

showed that combination of GHMT (Gata4, Hand2, Mef2c, and Tbx5) was no sufficient to reprogram human fibroblasts. They screened additional transcription factors and revealed that adding Myocd to GHMT significantly increased $cTnT^+$ iCMs from neonatal and adult human fibroblasts. Moreover, addition of miR1 and miR133 further enhanced reprogramming and eliminated the requirement for Mef2c. 8 weeks after transduction of 6 factors into adult human cardiac fibroblasts (CFs), iCMs showed spontaneous calcium oscillations and a small portion of iCMs spontaneously contracted 11 weeks after transduction of 6 factors.

Wada et al [22] reported that GMT was not sufficient for human cardiac reprogramming and addition of Myocd and Mesp1 to GMT (GMTMM) was sufficient to convert human cardiac and dermal fibroblasts into iCMs. They showed that around 5% of iCMs from CFs with GMTMM expressed cTnT and a-actinin. Moreover, iCMs showed increased cardiac and decreased fibroblast gene expression. aSMA staining in iCMs revealed that a-actinin-positive iCMs were positive for aSMA, a marker of embryonic cardiomyocytes, meaning that iCMs are mostly immature type cardiomyocytes.

We reported that addition of Esrrg and Mesp1 to GMT (5F) reprogrammed human fibroblasts into iCMs [23]. We utilized a transgenic H9 human ESC line carrying mCherry under the promoter of aMHC gene. We then differentiated aMHC-mCherry hESCs into fibroblasts and used as a cell source for reprogramming. We selected 13 transcription factors and 3 growth factors and transduced them all into fibroblasts along with GMT factors. GMT + 16 factors induced aMHC-$mCherry^+$ iCMs. By eliminating inhibitory and unnecessary factors, we found that a minimal combination of Esrrg, Mesp1 and GMT was sufficient to induce aMHC and cTnT double-positive iCMs. Moreover, addition of two more factors, Myocd and ZFPM2, to 5F combination (7F) further increased iCM yield. iCMs with either 5F or 7F showed calcium transients and resting membrane potential similar to that of adult CMs and global gene expression shifted from fibroblasts to cardiomyocyte-like state, however, did not spontaneously contracted. More recently, Mohamed et al [24] added TGF-b and Wnt signaling inhibitors to 7F combination and induced 50% of 7F-transduced human CFs into iCMs with

spontaneous calcium oscillations while 7F by itself showed less than 5% of cells with calcium oscillations.

1.3. CELL CYCLE IN EPIGENETIC REPROGRAMMING

1.3.1. Cell Cycle in iPSC Reprogramming

Chen et al [25] synchronized human dermal fibroblasts (HDFs) at G1 phase by serum-free media prior to induction of iPSCs and showed increased portion of TRA1-60^{+} 15-20 folds compared to unsynchronized HDFs. Synchronization of HDFs increased retroviral infection efficiency and increased mesenchymal to epithelial transition (MET), which is one essential event during epigenetic reprogramming of cells. Moreover, iPSCs generated with synchronization had no loss in pluripotency marker expression and differentiation ability in vitro.

1.3.2. Cell Cycle in Induced-neuron Reprogramming

Jiang et al [26] synchronized human fetal lung fibroblast MRC5 (Medical Research Council 5) at G1 phase by various methods of synchronization, including serum-free media, and significantly improved reprogramming of TH^{+} or Tuj1^{+} induced dopaminergic (iDA) neurons in vitro. On the other hand, their study showed that iDA neurons rapidly exit cell cycle upon reprogramming induction, within 24 hours of reprogramming induction, and majority of EdU^{+} proliferating cells failed to be reprogrammed, suggesting that cell cycle exit is an essential process for reprogramming of iDA neurons.

1.4. REFERENCES

[1] Choi J, Costa ML, Mermelstein CS, Chagas C, Holtzer S, Holtzer H (1990) MyoD converts primary dermal fibroblasts, chondroblasts, smooth muscle, and retinal pigmented epithelial cells into striated mononucleated myoblasts and multinucleated myotubes. Proc Natl Acad Sci U S A 87:7988–92.

[2] Takahashi K, Yamanaka S. Induction of pluripotent stem cells from mouse embryonic and adult fibroblast cultures by defined factors. Cell. 2006;126:663–76.

[3] Takahashi K, Tanabe K, Ohnuki M, Narita M, Ichisaka T, Tomoda K, et al. Induction of pluripotent stem cells from adult human fibroblasts by defined factors. Cell. 2007;131:861–72.

[4] Ieda M, Fu JD, Delgado-Olguin P, Vedantham V, Hayashi Y, Bruneau BG, Srivastava D. Direct reprogramming of fibroblasts into functional cardiomyocytes by defined factors. Cell. 2010;142:375–86.

[5] Song K, Nam YJ, Luo X, Qi X, Tan W, Huang GN, Acharya A, Smith CL, Tallquist MD, Neilson EG, Hill JA, Bassel-Duby R, Olson EN. Heart repair by reprogramming non-myocytes with cardiac transcription factors. Nature. 2012;485:599–604.

[6] Protze S, Khattak S, Poulet C, Lindemann D, Tanaka EM, Ravens U (2012) A new approach to transcription factor screening for reprogramming of fibroblasts to cardiomyocyte-like cells. J Mol Cell Cardiol 53(3):323–332

[7] Addis RC, Ifkovits JL, Pinto F, Kellam LD, Esteso P, Rentschler S, Christoforou N, Epstein JA, Gearhart JD (2013) Optimization of direct fibroblast reprogramming to cardiomyocytes using calcium activity as a functional measure of success. J Mol Cell Cardiol 60:97–106

[8] Hirai H, Katoku-Kikyo N, Keirstead SA, Kikyo N (2013) Accelerated direct reprogramming of fibroblasts into cardiomyocyte-like cells with the MyoD transactivation domain. Cardiovasc Res 100(1):105–113

[9] Jayawardena TM, Egemnazarov B, Finch EA, Zhang L, Payne JA, Pandya K, Zhang Z, Rosenberg P, Mirotsou M, Dzau VJ (2012) MicroRNA-mediated in vitro and in vivo direct reprogramming of cardiac fibroblasts to cardiomyocytes. Circ Res 110(11):1465–1473

[10] Muraoka N, Yamakawa H, Miyamoto K, Sadahiro T, Umei T, Isomi M, Nakashima H, Akiyama M, Wada R, Inagawa K, Nishiyama T, Kaneda R, Fukuda T, Takeda S, Tohyama S, Hashimoto H, Kawamura Y, Goshima N, Aeba R, Yamagishi H, Fukuda K, Ieda M (2014) MiR-133 promotes cardiac reprogramming by directly repressing Snai1 and silencing fibroblast signatures. EMBO J 33(14):1565–1581

[11] Wang H, Cao N, Spencer CI, Nie B, Ma T, Xu T, Zhang Y, Wang X, Srivastava D, Ding S (2014) Small molecules enable cardiac reprogramming of mouse fibroblasts with a single factor. Cell Rep 6(5):951–960

[12] Fu Y, Huang C, Xu X, Gu H, Ye Y, Jiang C, Qiu Z, Xie X (2015) Direct reprogramming of mouse fibroblasts into cardiomyocytes with chemical cocktails. Cell Res 25(9):1013–1024

[13] Cao N, Huang Y, Zheng J, Spencer CI, Zhang Y, Fu JD, Nie B, Xie M, Zhang M, Wang H, Ma T, Xu T, Shi G, Srivastava D, Ding S (2016) Conversion of human fibroblasts into functional cardiomyocytes by small molecules. Science 352(6290):1216–1220

[14] Ifkovits JL, Addis RC, Epstein JA, Gearhart JD (2014) Inhibition of TGFbeta signaling increases direct conversion of fibroblasts to induced cardiomyocytes. PLoS One 9(2):e89678

[15] Zhao Y, Londono P, Cao Y, Sharpe EJ, Proenza C, O'Rourke R, Jones KL, Jeong MY, Walker LA, Buttrick PM, McKinsey TA, Song K (2015) High-effciency reprogramming of fibroblasts into cardiomyocytes requires suppression of pro-fibrotic signalling. Nat Commun 6:8243

[16] Zhou H, Dickson ME, Kim MS, Bassel-Duby R, Olson EN (2015) Akt1/protein kinase B enhances transcriptional reprogramming of fibroblasts to functional cardiomyocytes. Proc Natl Acad Sci USA 112(38):11864–11869

[17] Yamakawa H, Muraoka N, Miyamoto K, Sadahiro T, Isomi M, Haginiwa S, Kojima H, Umei T, Akiyama M, Kuishi Y, Kurokawa J, Furukawa T, Fukuda K, Ieda M (2015) Fibroblast growth factors and vascular endothelial growth factor promote cardiac reprogramming under defined conditions. Stem Cell Reports 5(6):1128–1142

[18] Wang, Liu, Yin, Asfour, Chen, Li, Bursac, Liu, Qian (2015) Stoichiometry of Gata4, Mef2c, and Tbx5 Influences the Efficiency and Quality of Induced Cardiac Myocyte Reprogramming. *Circulation Research* 116:237–244.

[19] Liu Z, Chen O, Zheng M, Wang L, Zhou Y, Yin C, Liu J, Qian L (2016) Re-patterning of H3K27me3, H3K4me3 and DNA methylation during fibroblast conversion into induced cardiomyocytes. Stem Cell Res 16(2):507–518

[20] Zhou Y, Wang L, Vaseghi HR, Liu Z, Lu R, Alimohamadi S, Yin C, Fu JD, Wang GG, Liu J, Qian L (2016) Bmi1 is a key epigenetic barrier to direct cardiac reprogramming. Cell Stem Cell 18(3):382–395

[21] Nam YJ, Song K, Luo X, Daniel E, Lambeth K, West K, Hill JA, DiMaio JM, Baker LA, Bassel-Duby R, Olson EN (2013) Reprogramming of human fibroblasts toward a cardiac fate. Proc Natl Acad Sci USA 110(14):5588–5593

[22] Wada R, Muraoka N, Inagawa K, Yamakawa H, Miyamoto K, Sadahiro T, Umei T, Kaneda R, Suzuki T, Kamiya K, Tohyama S, Yuasa S, Kokaji K, Aeba R, Yozu R, Yamagishi H, Kitamura T, Fukuda K, Ieda M (2013) Induction of human cardiomyocyte-like cells from fibroblasts by defined factors. Proc Natl Acad Sci USA 110(31):12667–12672

[23] Fu JD, Stone NR, Liu L, Spencer CI, Qian L, Hayashi Y, Delgado-Olguin P, Ding S, Bruneau BG, Srivastava D (2013) Direct reprogramming of human fibroblasts toward a cardiomyocyte-like state. Stem Cell Reports 1(3):235–247

[24] Mohamed TM, Stone NR, Berry EC, Radzinsky E, Huang Y, Pratt K, Ang YS, Yu P, Wang H, Tang S, Magnitsky S, Ding S, Ivey KN, Srivastava D (2016) Chemical enhancement of in vitro and in vivo direct cardiac reprogramming. *Circulation* 135.10: 978-995 doi:10.1161/CIRCULATIONAHA.116.024692

[25] Chen M, Huang J, Yang X, Liu B, Zhang W, Huang L, Deng F, Ma J, Bai Y, Lu R, Huang B, Gao Q, Zhuo Y, Ge J. Serum starvation induced cell cycle synchronization facilitates human somatic cells reprogramming. *PLoS ONE*. 2012; 7:e28203.

[26] Jiang H, Xu Z, Zhong P, Ren Y, Liang G, Schilling H, Hu Z, Zhang Y, Wang X, Chen S, Yan Z, Feng J. Cell cycle and p53 gate the direct conversion of human fibroblasts to dopaminergic neurons. *Nat Commun*. 2015; 6:10100.

CHAPTER 2

S-PHASE SYNCHRONIZATION FACILITATES THE EARLY PROGRESSION OF INDUCED-CARDIOMYOCYTE REPROGRAMMING THROUGH ENHANCED CELL-CYCLE EXIT

2.1. ABSTRACT

Rationale: Direct reprogramming of fibroblasts into induced cardiomyocytes (iCMs) holds a great promise for cardiac regenerative medicine. However, low conversion rate and immaturity remain as the main hurdles. Generating more mature and quality iCMs underlies a better mechanistic understanding of the reprogramming process. Cell cycle regulation, a general mechanism of the cells, has not been well understood in iCMs.

Objective: We proposed to research how proliferation and cell cycle exit are involved in iCM reprogramming.

Methods and Results: We utilized αMHC-GFP transgene to follow up live progress of reprogramming. Serial pictures of immature αMHC-GFP^{+} iCMs at DPI-2-4 (post-infection days) revealed that approximately half of the cells proliferated after turning on αMHC-GFP reporter and this rate decreased gradually until they all finally exit cell cycle at DPI-21. Moreover, transient cell cycle arrest at S and G2/M phases in immature iCMs facilitated cell cycle exit and diminished cell cycle marker gene expression. Early onset of cell cycle exit through cell cycle synchronizing drugs decreased the yield of αMHC-GFP^{+} iCMs, yet improved expression levels of essential cardiac genes. On the other hand, a single polycistronic construct of reprogramming factors (MGT) with P2A and T2A sequences limited proliferation capability of αMHC-GFP^{+} iCMs and facilitated cell cycle exit in earlier stages. MGT, similarly, decreased cell cycle gene expression, yet improved cardiac gene expression in αMHC-GFP^{+} iCMs. Interestingly, we found that GFP^{high} population of iCMs exhibited improved cardiac gene expression and decreased cell cycle and proliferation gene expression compare to GFP^{low} iCMs. MGT reprogrammed a bigger portion of MEFs into GFP^{high} iCMs. This assured that GFP^{high} cell population is a more desired form of iCMs.

Conclusions: Our results indicate that proliferation is undesired for iCM maturation, and cell cycle exit at earlier stages of reprogramming is beneficial for maturation of iCMs. A better understanding of cell cycle exit in iCMs will help generating more mature and functional iCMs.

2.2. BRIEF BACKGROUND

Cardiomyocytes (CMs) in the adult heart have limited regenerative capacity (**Van Berlo and Molkentin, 2014**). At the onset of heart disease, lost CMs are typically replaced with fibrotic scar tissue, subsequently leading to chronic heart failure, which remains one of the leading causes of death worldwide. Recent studies have found that mouse (**Ieda et al., 2010; Jayawardena et al., 2012; Song et al., 2012; Qian et al., 2012**) and human (**Fu et al., 2013; Nam et al., 2013; Wada et al., 2013**) fibroblasts can be directly reprogrammed into induced CMs (iCMs), which holds a great promise for the development of a new therapeutic approach for heart disease. In order to improve induction efficiency and quality of iCMs, studies have focused on developing optimized reprogramming methods and investigating the mechanism of direct cardiac reprogramming, including the use of polycistronic vectors for an optimal stoichiometry of reprogramming factors (**Wang et al., 2015**), suppression of critical epigenetic barriers (**Zhou et al., 2015; Zhou et al., 2016**) and pro-fibrotic signaling (**Muraoka et al., 2014; Ifkovits et al., 2014; Zhao et al., 2015),** optimization of culture conditions (**Yamakawa et al, 2015; Mohamed et al., 2017**), and suppression of inflammatory process (**Zhou et al., 2017a**). However, the cell-cycle regulation, a fundamental biological process, has not been investigated during iCM-reprogramming.

Similar to fully differentiated adult CMs, it has been recognized that reprogrammed iCMs exit the cell cycle. No cardiac troponin-T $(cTnT)^+$ iCMs were positively stained with Ki67 at week-2 of reprogramming (**Addis et al., 2013);** 5-ethynyl-20-deoxyuridine (EdU) assay didn't show any EdU^+ iCMs from week-2 to week-4 post-induction (**Yamakawa et al., 2015**). More recently, none of the α-$Actinin^+$ iCMs expressed proliferation marker, Ki67, at DPI-28 (**Zhou et al., 2017b**). These studies indicate that cell cycle exit is an important event happening during the process of iCM-reprogramming; however, it is unknown whether cell-cycle exit of reprogrammed iCMs happens right upon reprogramming induction or at a later stage of reprogramming process. A cell cycle constitutes a critically important chain of interconnected events with a dynamic fluctuation of epigenetic chromatin modifications (**Bou Kheir and Lund, 2010**), including genomic DNA methylation and histone

modification, which have significant influence on epigenetic reprogramming of somatic cell fate (**Buganim et al., 2013**). Indeed, it has been reported that pre-synchronization of fibroblasts at the G0/G1-phase by transient serum starvation could significantly improve the reprogramming yield of induced pluripotent stem cells (iPSCs) (**Chen et al., 2012**). In addition, cell-cycle pre-synchronization at the G1-phase could markedly enhance the reprogramming efficiency of induced dopaminergic neurons (**Jiang et al., 2015**). These studies suggested that manipulation of cell-cycle progression has a significant impact on epigenetic reprogramming; however, it is unknown in which cell-cycle phase epigenetic iCM-reprogramming is initiated in fibroblasts and if manipulating the cell cycle (i.e. synchronization) of post-infected fibroblasts influences the progression of reprogramming.

In this study, we first performed 48-hour time-lapse recordings to monitor the early progression of iCM-reprogramming and found that αMHC-GFP^{+} iCMs went through cell division at the early stage of reprogramming and exited cell cycle along the process of reprogramming. iCM-reprogramming was majorly initiated at late-G1- or S- phase. We also synchronized cell cycle of reprogramming fibroblasts at various time points post GMT-retrovirus infection and found that S-phase synchronization at day 1 post-infection (DPI-1) facilitated cell-cycle exit of reprogrammed iCMs and accelerated the early progression of reprogramming.

2.3. METHODS

2.3.1. Mouse Embryonic Fibroblast (MEF) Isolation

Transgenic mouse line overexpressing GFP (green fluorescent protein) under αMHC (α-myosin heavy chain) gene promoter was defined by **Ieda et al (2010)**. Embryonic fibroblasts were prepared from E12.5-13.5 αMHC-GFP^{+} embryos. GFP expressing embryos were collected under sterile conditions, briefly washed in 70% Ethanol, and extensively washed in 1X PBS, followed by removal of internal organs and head. Remaining parts of embryos were washed in PBS and chopped into small pieces (1-2mm^3) prior to enzyme digestion. Tissue pieces were digested in 2ml of 0.125% Trypsin/EDTA per embryo at 37^{o}C water bath for 20min. After every 5min, tissue pieces were pipetted up and down 5-10 times. 2-3ml of 0.25% Trypsin/EDTA was added and incubated for another 5-10min until most tissue was dissociated well in trypsin. Trypsin was quenched with equal amount of medium with 10%FBS (HyClone, ThermoScientific). Cells were filtered through a 40μM cell strainer (Falcon) and centrifuged at 1500rpm for 3min. Pellet was dissolved in DMEM medium with 10% heat-inactivated FBS, cultured at 37^{o}C, 5%CO_2 until full confluence, and used freshly or preserved at -80^{o}C freezer for short-term or in liquid nitrogen for long-term storage.

2.3.2. Cell Culture and Reprogramming

PlatE packaging cells were cultured in PlatE medium containing high glucose DMEM with 10% FBS and selected with 1μg/ml puromycin (Gibco) and 10μg/ml blasticidin (Gibco). 24hrs before transfection, 2.5x10^6 cells per 6 cm dish were plated in PlatE medium without selection antibiotics. 3ug pMX retroviral plasmids of Gata4, Mef2c, and Tbx5 (GMT) plasmids (**Ieda et al., 2010**) or polycistronic Mef2c-Gata4-Tbx5 (MGT) plasmid expressing P2A and T2A cleavage peptide sites (**Wang et al., 2015**) and 9uL of FugeneHD transfection reagent (Promega) were incubated in Opti-MEM media (Gibco) at room temperature for 20min. 24hrs after transfection, medium was refreshed with PlatE medium. Viruses were harvested 48hrs after transfection and filtered through 0.45uM low

protein-binding filters (Nalgene, ThermoScientific). MEFs were infected with 0.5ml MGT or 1.5 ml mixture of individual GMT viruses for 24hrs with 8ug/ml final concentration of polybrene (Millipore). The medium was changed into and thereafter maintained in cardiac reprogramming medium (DMEM/M199 (4:1) with 10% heat-inactivated FBS (Hyclone, ThermoScientific), NEAA (Gibco), and L-Glutamine (Gibco)). Media were changed every 2-3 days until iCMs were analyzed at either Day7 or Day10. For evaluation of reprogramming efficiency, the cells were harvested by 0.05% Trypsin/EDTA, dissolved in FACS buffer (2mM EDTA and 5%FBS in 1X PBS), and analyzed by BD Accuri C6 (BD Biosciences).

2.3.3. Cell Cycle Synchronization

iCMs were induced with monocistronic pMX GMT constructs as described and synchronized for 24hrs using 2mmol/L Thymidine (T9250, Sigma) , 25umol/L Lovastatin (1370600, Sigma), 50ng/ml Nocodazole (M1404, Sigma), 2ug/ml Aphidicoline (A0781, Sigma), 2mmol/L Hydroxyurea (H8627, Sigma), 0.5mmol/L L-Mimosine (M0253, Sigma) or FBS-free cardiac reprogramming media. Next day, cells were extensively washed with 1X PBS to remove the drugs and fresh cardiac reprogramming media was added on cells. Cells were maintained in cardiac reprogramming media by refreshing media every 2-3 days until flow cytometry or qPCR analysis.

2.3.4. Time Lapse Imaging of αMHC-GFP$^+$ iCMs

Cardiac reprogramming was induced as described using either GMT or MGT. Cell media was refreshed prior to time-lapse imaging. At DPI-2, sequential pictures of infected MEFs were recorded for 48hrs using DMi8 Leica fluorescent microscope (Leica Microsystems). To allow observation of transition from GFP$^-$ to GFP$^+$ stage, the camera was focused on GFP$^-$ areas at DPI-2. Recorded pictures were analyzed by MetaMorph software (Molecular Devices) to assess proliferation of iCMs. Video files for images with bright field and GFP fluorescence were individually prepared in MetaMorph and joined together side-to-side to obtain a single video file.

2.3.5. EdU Assay and Cell Cycle Analysis

Plain MEFs were labeled with 10mM EdU for 2hrs or iCMs for 24hrs in MEF media containing high glucose DMEM and heat-inactivated FBS before collecting the cells for staining. The cells were washed with 1X PBS, harvested in 0.05% Trypsin/EDTA, and pelleted at 1500rpm for 3min. Cells in pellet were fixed in 4% PFA for 15min at RT. PFA was removed by extensive washing of pellet with 1X PBS. Cells were resuspended in 1X saponin solution and respectively stained with anti-EdU antibodies and nuclear staining solution (40ug Propidium Iodide (P4170, Sigma), 100ug RNaseA (ThermoScientific) in final volume of 500uL) by using Click-iT Plus Flow Cytometry Assay protocol (Life Technologies). iCMs were additionally stained with GFP-FITC antibodies (1:100) (NB100-1771, Novus Biologicals) as recommended by Click-iT protocol. Cells were filtered through a cell strainer and analyzed by BD Accuri C6 (BD Biosciences).

2.3.6. Western Blot Analysis

iCMs were generated as described, harvested by 0.05% trypsin, washed by PBS, and lysed in lysis buffer (1% Triton X-100, 150mmol/L NaCl, 50mmol/L TrisHCl pH7.5, 1mmol/L EDTA). To allow complete lysis of cells, cells were incubated on ice for 20-30 min. Proteins were separated in SDS-PAGE gels, transferred to nitrocellulose membranes, and stained with anti-Gata4 (1:5000, sc-1237, SantaCruz), anti-Mef2c (1:5000, ARP37342_T100, Aviva Systems Biology), anti-Tbx5-Flag (1:500, PA1-984B, ThermoScientific), and β-Actin (1:1000, A1978, Sigma) or GAPDH (1:1000, sc-166545, Santa Cruz) on individual blots. Pierce ECL Plus chemiluminescence detection kit (Thermo Scientific) was used to detect the proteins.

2.3.7. Pre-amplification of Genes and qRT-PCR

iCMs were harvested by 0.05% trypsin, filtered through a cell strainer, and resuspended in FACS buffer. GFP^+ iCMs were sorted by HAPS1 cell sorter (iCyt, Sony). Cells were lysed in 10uL resuspension buffer and 1uL lysis enhancer from CellsDirect One-step qRT-PCR Kit (Invitrogen). To complete lysis, cells were heated at 75^{o}C for 10min in a thermal cycler. Preamplification primer mix was prepared by mixing all primers in a single tube at 0.5uM final concentration for each primer. After the lysis, the genes of interest (**Table1**) were pre-amplified by pre-amplification primer mix in a thermal cycler as recommended by CellsDirect One-step qRT-PCR kit. The pre-amplified genes were further amplified by SsoFast Evagreen supermix (Biorad) with individual primer sets in 7300 real-time PCR system (Applied Biosystems).

2.3.8. Statistical Analyses

All data were analyzed with at least three biological replicates and expressed as mean ± SEM unless specified in figure legends. The statistical significance was examined by two-way paired or unpaired student's t-test or ANOVA. p-value of less than 0.05 was regarded as statistically significant.

2.4. RESULTS

2.4.1. iCMs go through cell division and exit cell cycle along with the progress of reprogramming

For iCM reprogramming, we infected αMHC-GFP transgenic mouse embryonic fibroblasts (MEFs) with a cocktail of Gata4, Mef2c, and Tbx5 (GMT) retroviruses and found that GFP could be first observed from DPI-2, which was consistent with the observation that a high-level overexpression of GMT was achieved around 48 hours post-infection (**Figure 1**). In order to determine if cell division occurs during iCM-reprogramming, we recorded a 48-hour time-lapse at DPI-2 through DPI-4 to monitor the activation of αMHC-GFP during the early progression of iCM-reprogramming (**Figure 2A**). We purposely set a three-second exposure time for GFP recording to recognize very faint GFP fluorescence, indicative of initial activation of αMHC-GFP (**Figure 2A, frame** İ); we found that the fluorescence of αMHC-GFP was gradually enhanced during the process of reprogramming. Surprisingly, we found that ~41% (39 out of 95) of αMHC-GFP^{+} primary GMT-reprogrammed iCMs (GMT-iCMs) underwent cell division once within the 48-hour recording time (**Figure 2A and 2B**). Noticeably, ~16% (22 out of 134) of GMT-iCMs died before or after cell division (**Figure 2B**). Our time-lapse recordings revealed that iCMs at the early stage of reprogramming could still actively divide.

We next performed an EdU assay to quantify cell division of αMHC-GFP^{+} iCMs from DPI-4 to later stages of the reprogramming process. Consistent with our previous study (**Ieda et al., 2010**), the percentage of reprogrammed-αMHC-GFP^{+} iCMs gradually increased from DPI-4 to DPI-7, then decreased after two weeks (**Figure 2C-2D**). We then incubated retrovirus-infected MEFs with EdU for 24 hours to label all the dividing cells within that time; we found that more than 80% of uninfected MEFs divided within 24 hours (**Figure 2E**). Noticeably, 30.8±3.5% of GMT-iCMs at DPI-4 were dividing and positively stained for EdU, which is consistent with our time-lapse results (DPI-2 to DPI-4). Furthermore, the percentage of EdU^{+}-iCMs gradually decreased from DPI-4 to DPI-21 and

almost none of the αMHC-GFP$^+$ iCMs at DPI-21 were stained positively for EdU (**Figure 2F**), indicating that all iCMs, which were αMHC-GFP$^+$/EdU$^-$, had exited cell cycle at this late stage of reprogramming. Consistent with our study, none of the α-Actinin$^+$ iCMs at DPI-28 expressed proliferation marker, Ki67 (**Zhou et al., 2017b**).

2.4.2. iCM-reprogramming can be initiated in all three phases of cell cycle

We next asked in which phase of the cell cycle is iCM-reprogramming initiated. To answer this question, we carefully calculated the time between two consecutive cell divisions of MEFs in our time-lapse recordings and estimated that MEFs had an average of 25.3±7.4 hours of cell-cycle length (n=42, **Figure 3A**). We performed EdU assay with two-hour EdU-labelling and measured the average percentages of G1 (~60%), S (~29%), and G2/M (~11%) in MEFs (**Figure 3B and 3C**, n=4), which represent the percentages of the time spent in each phase out of whole cell-cycle duration (**Wieder et al., 1990**). Therefore, the duration of G1 phase was calculated as ~15.2 hours (~60% of 25.3 hours), S phase ~7.3 hours, and G2/M phase ~2.8 hours (**Figure 3D**). We then measured the time from the completed cell-division back to the first appearance of the αMHC-GFP reporter (**Figure 3E**) and determined in which cell-cycle phase reprogramming of individual iCMs was initiated. For example, the reprogramming initiation of one iCM in **Figure 2A** (indicated by arrow head) was started from 15 minutes with the first appearance of faint GFP-fluorescence (**Figure 2A**, frame İ) and cell division happened at 21 hours (**Figure 2A**, frame V); therefore, reprogramming of this iCM was initiated at G1 phase and took 20.75 hours to pass through G1 (10.65 hours), S (7.3 hours), and G2/M (2.8 hours) phases for a completion of cell division. These transition times from reprogramming initiation to cell division of GMT-iCMs (n=34, **Figure 3E**) were converted into a distribution chart of cell-cycle phases (**Figure 3F**). We found that 23 iCMs initiated the activation of αMHC-GFP at G1-phase, including 15 at late G1-phase, 10 at S-phase, and 2 at early G2-phase (**Figure 3E**), demonstrating that iCM-reprogramming were mostly initiated at late G1- and S phases.

2.4.3. S- or G2/M-phase synchronization at DPI-1 facilitates cell-cycle exit of GMT-iCMs

Since the epigenetic status dynamically fluctuates throughout the cell cycle (Bou Kheir et al., 2010), we then investigated if synchronizing a specific cell-cycle phase in GMT-infected fibroblasts could improve iCM-reprogramming. At DPI-1, GMT-infected MEFs were synchronized at G1-, G0/G1-, G1/S-, or G2/M-phase, by a 24-hour incubation with lovastatin, serum-free media, thymidine, or nocodazole for 24 hours (**Figure 4A**), respectively; the morphology of synchronized MEFs displayed cell-cycle related changes (**Figure 5**), as previously reported (**Rosner et al., 2013**). We found that thymidine-induced G1/S-synchronization could increase the percent yield of reprogrammed αMHC-GFP$^+$ iCMs, while lovastatin-induced G1 synchronization had no significant influence (**Figure 4B and 4C).** However, the absolute number (i.e. yield) of αMHC-GFP$^+$ iCMs was not significantly improved by thymidine-synchronization (**Figure 4C**) but was dramatically decreased by G2/M-synchronization of nocodazole.

We next investigated the effect of S-phase synchronization, mediated by aphidicolin, hydroxyurea, or L-mimosine (**Figure 6**) as previously reported (Ma et al., 2011), on iCM-reprogramming and found that all three compounds significantly suppressed iCM-reprogramming with decreased percentage and absolute number of αMHC-GFP$^+$ iCMs (**Figure 4D)**. Interestingly, iCM-reprogramming was inhibited by S-phase synchronization only at DPI-1 but not at DPI-2 to DPI-6 (**Figure 7**), indicating that DPI-1 is a critical time window for regulating iCM-reprogramming. Importantly, none of the synchronizations at DPI-1 inhibited the protein expressions of GMT in infected MEFs (**Figure 7D**). While un-reprogrammed MEFs could quickly recover from cell-cycle arrest and reenter cell cycle 24 hours after removing compounds (**Figure 8**), we found that S- or G2/M-synchronization, but not G1-synchronization, at DPI-1 significantly decreased the percentage of dividing EdU$^+$/αMHC-GFP$^+$ GMT-iCMs at DPI-7 (**Figure 4E**). Our data suggested that S- or G2/M- synchronization at DPI-1 promoted cell-cycle exit in GMT-reprogrammed iCMs.

2.4.4. S-phase synchronization accelerates the early progression of iCM-reprogramming through enhanced cell-cycle exit

Our time-lapse recordings showed that iCMs initially expressed a low amount of αMHC-GFP (GFP^{low}) and gradually turned into brighter GFP^+ cells (GFP^{high}) along with the progress of reprogramming (**Figure 2A**), which was disclosed with varying intensities of GFP fluorescence across iCMs by FACS assay (**Figure 9A**), suggesting that the intensity of GFP fluorescence might indicate different progress of reprogramming achieved in individual iCMs. We then gated all reprogrammed-αMHC-GFP^+ cells at DPI-2, which were newly reprogrammed in theory, as a GFP^{low} sub-population (**Figure 9A**) and gated remaining αMHC-GFP^+ cells with more intense GFP-fluorescence as a GFP^{high} sub-population. We found that GFP^{high} iCMs covered a significantly bigger portion of αMHC-GFP^+ iCMs that exited cell cycle than the GFP^{low} population, indicated by smaller portion of EdU^+ iCMs (**Figure 9B**). We then sorted out GFP^{low} and GFP^{high} populations and found that, compared to GFP^{low} cells, GFP^{high} iCMs expressed many cardiac genes at a significantly higher level, including *Atp2a2, Myl7, Actc1*, and *Ryr2* (**Figure 9C and Figure 10**). Consistent with our EdU assay, the expression of *Mki67,* a proliferation marker gene, was significantly lower in GFP^{high} cells (**Figure 9C**). These results demonstrated that a more advanced reprogramming had been achieved in GFP^{high} iCMs. Importantly, S-phase synchronization at DPI-1 significantly increased the portion of GFP^{high} iCMs at DPI-7 (n=6, **Figure 9D**), suggesting that S-phase synchronization at DPI-1 accelerates the early progression of GMT-reprogramming.

It has been reported that a polycistronic construct (MGT), expressing an optimal stoichiometry of three reprogramming factors, could yield a better efficiency and a better quality of iCM-reprogramming in mouse cardiac fibroblasts than GMT monocistronic constructs (**Wang et al., 2015**). We found that GMT- and MGT-reprogramming of MEFs yielded a similar number of iCMs at DPI-3 through DPI-10 (**Figure 9E**). Our 48-hour time-lapse recordings also captured cell division and cell death in MGT-reprogrammed iCMs (MGT-iCMs) from DPI-2 to DPI-4 (**Figure 11**); however, the number of dividing cells was significantly less in MGT-iCMs than in GMT-iCMs (**Figure 9F**). Consistently, there were significantly less EdU^+ cells in MGT-iCMs than in GMT-iCMs within the first two weeks of reprogramming (**Figure 9G**); moreover, MGT-reprogramming was processed

faster and yielded significantly higher portion of GFP^{high} iCMs than GMT-reprogramming at DPI-7 and DPI-10 (**Figure 9H**). These results demonstrated that an advanced progression with enhanced cell-cycle exit was achieved in iCMs reprogrammed by polycistronic MGT. Importantly, S-phase synchronization failed to further increase the percentage of GFP^{high} population among MGT-iCMs (**Figure 9I**), suggesting that the facilitated progression of GMT-reprogramming by S-phase synchronization was mediated through a mechanism of accelerating cell-cycle exit (**Figure 12**).

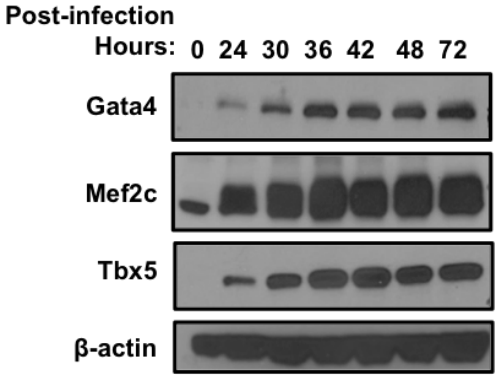

Figure 1. Reprogramming factors were highly expressed in MEFs 48 hours post retrovirus infection. A representative western blot image shows the expression of Gata4, Mef2c, and Tbx5 in MEFs at different post-infection hours.

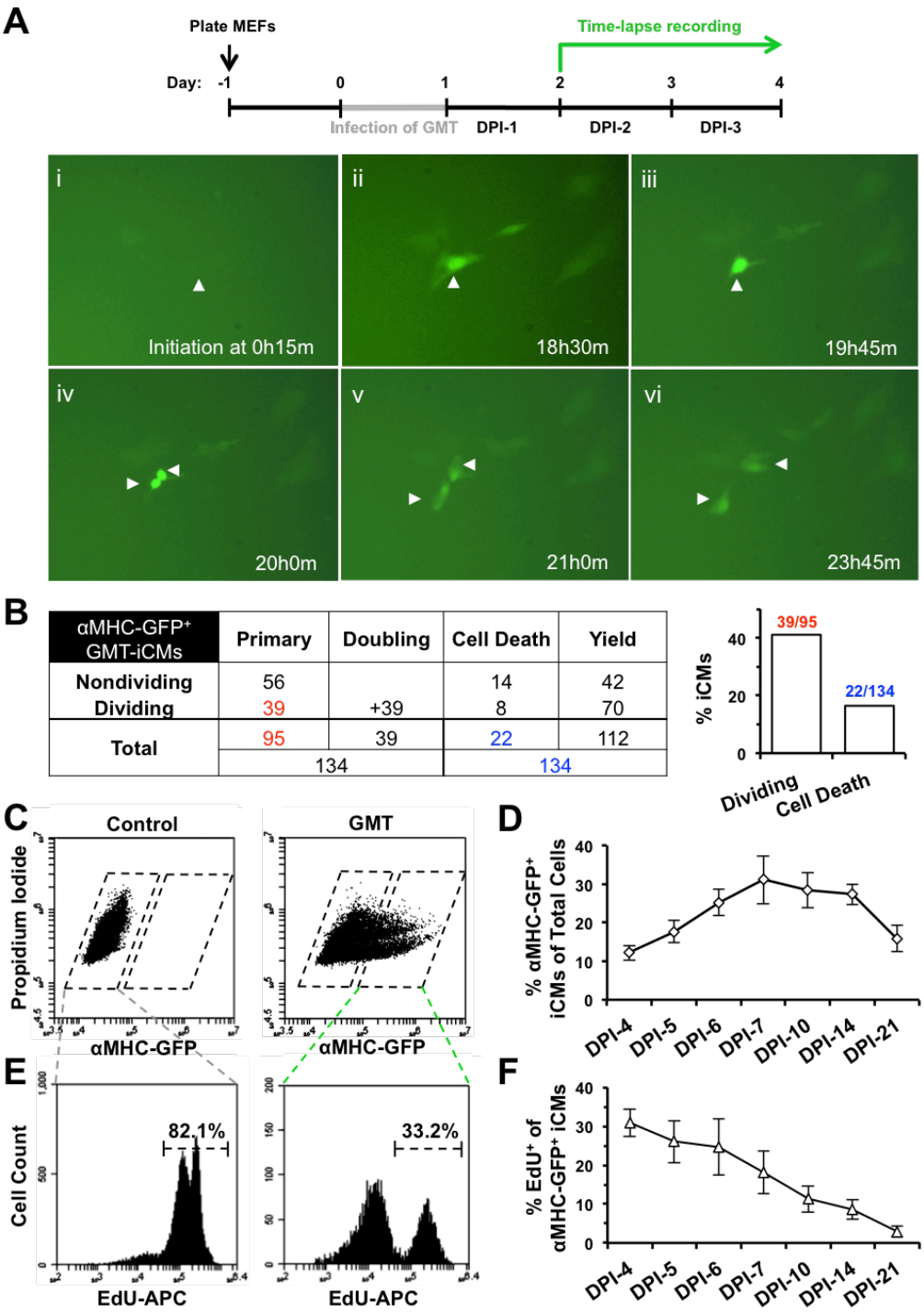

Figure 2. iCMs undergo cell division and exit cell cycle along the process of reprogramming. A) Representative images of a time-lapse recording showing that one primary GMT-iCM (arrowhead) divided into two daughter iCMs 20.75 hours after the activation of αMHC-GFP. A scale bar indicates 50μm. **B)** A table summarizing the time-lapse result of GMT-iCMs. Bar graph shows the percentage of dividing GMT-iCMs and iCMs that underwent cell death. **C)** Representative FACS plots of αMHC-GFP$^+$ iCMs at day 4 post-infection (DPI-4). **D)** The percentage of αMHC-GFP$^+$ GMT-iCMs from DPI-4 to DPI-21 (n=3). **E)** Representative FACS plots of 24-hour-incubation EdU assay assessing cell division of MEFs and αMHC-GFP$^+$ iCMs. **F)** Percentage of dividing EdU$^+$/αMHC-GFP$^+$ GMT-iCMs from DPI-4 to DPI-21 (n=5).

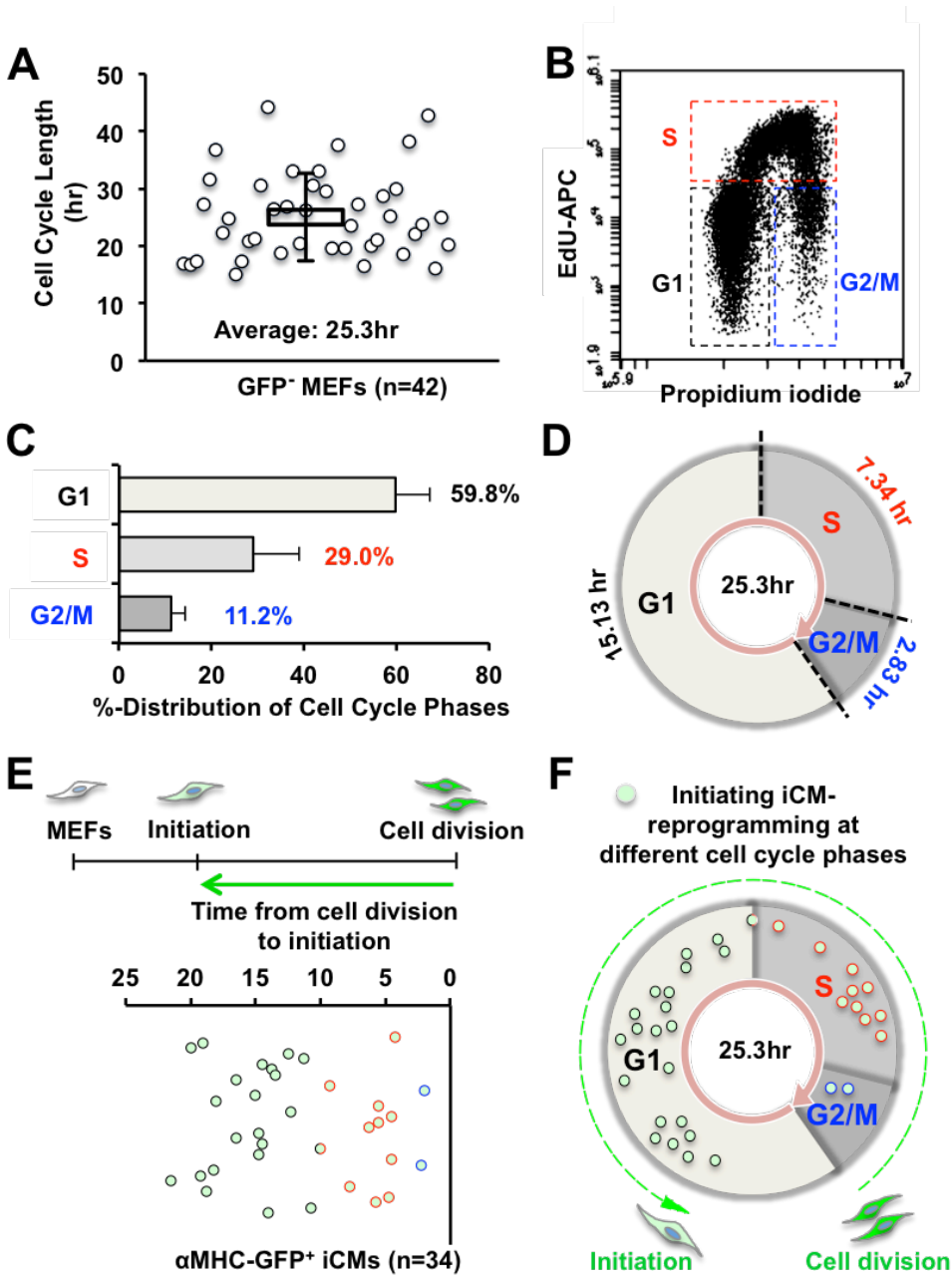

Figure 3. Cardiac reprogramming can be initiated at all three cell-cycle phases. A) Non-reprogrammed MEFs, which had two consecutive cell divisions in the time-lapse recordings, had an average of 25.3±7.4 hours cell-cycle length. **B)** Representative FACS plot of EdU assay with two-hour EdU-labeling showing a distribution of cell-cycle phases in MEFs. **C)** The average percentages of G1-, S-, and G2/M-phase in MEFs (n=4). **D)** MEFs had an average of 15.2-hour G1 phase, 7.3-hour S phase, and 2.8-hour G2/M phase. **E)** The time from the reprogramming-initiation to cell division in dividing GMT-iCMs (n=34). **F)** A distribution chart of cell-cycle phases in which reprogramming of those dividing iCMs (panel E) was initiated.

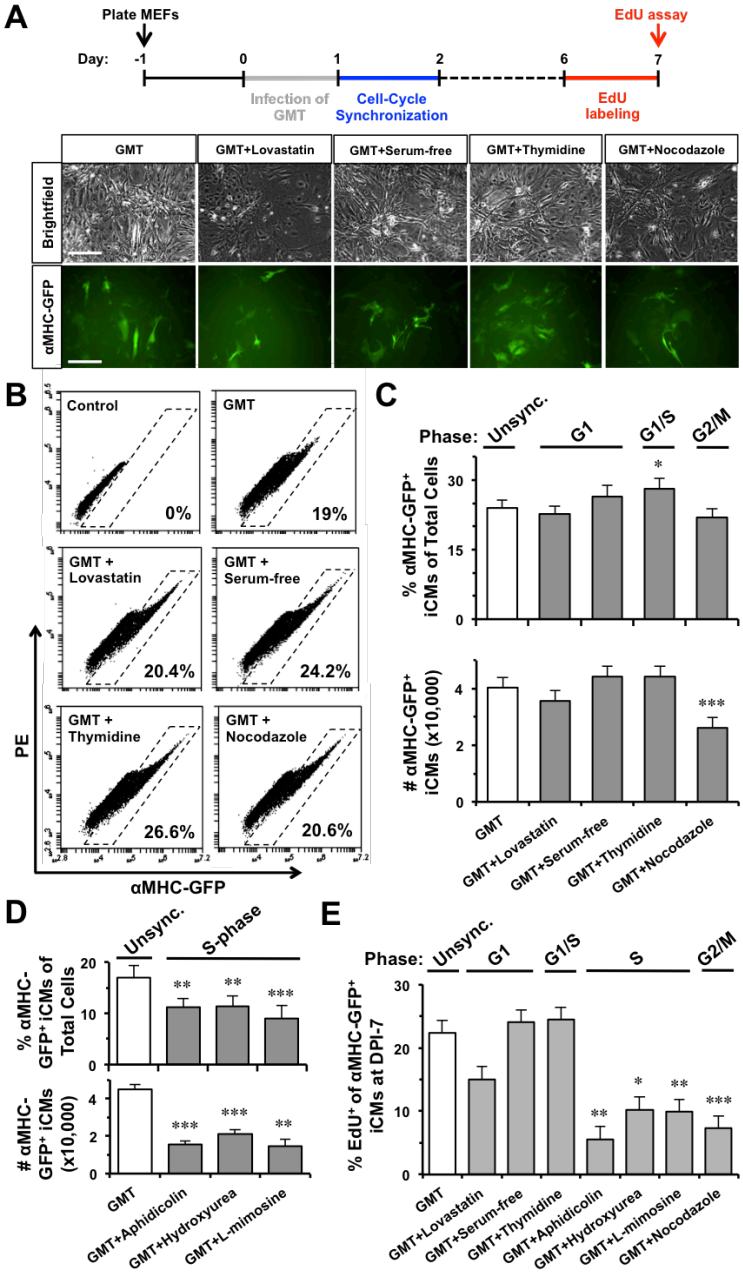

Figure 4. S- or G2/M-phase synchronization facilitates cell-cycle exit in GMT-reprogrammed iCMs. **A)** At DPI-1, MEFs were synchronized at G1, G0/G1, G1/S, or G2/M-phase by lovastatin, serum-free media, thymidine, or nocodazole, respectively. Representative pictures showing GMT-reprogrammed MEFs at DPI-10 with or without (Control) cell-cycle synchronization. Scale bars indicate 100μm. **B)** Representative FACS plots of reprogrammed αMHC-GFP^{+} iCMs at DPI-10. **C)** The effect of G1-, G1/S-, or G2/M-phase synchronization on GMT-iCMs (n=10), including the percentage (upper panel) and absolute number (lower panel) of αMHC-GFP^{+} iCMs. **D)** The effect of S-phase synchronization by aphidicolin, hydroxyurea, or L-mimosine on GMT-iCMs (n=5). **E)** The percentage of EdU^{+} cells in αMHC-GFP^{+} iCMs at DPI-7 with or without cell-cycle synchronization at DPI-1 (n=3). *p<0.05, **p<0.01 vs. GMT group.

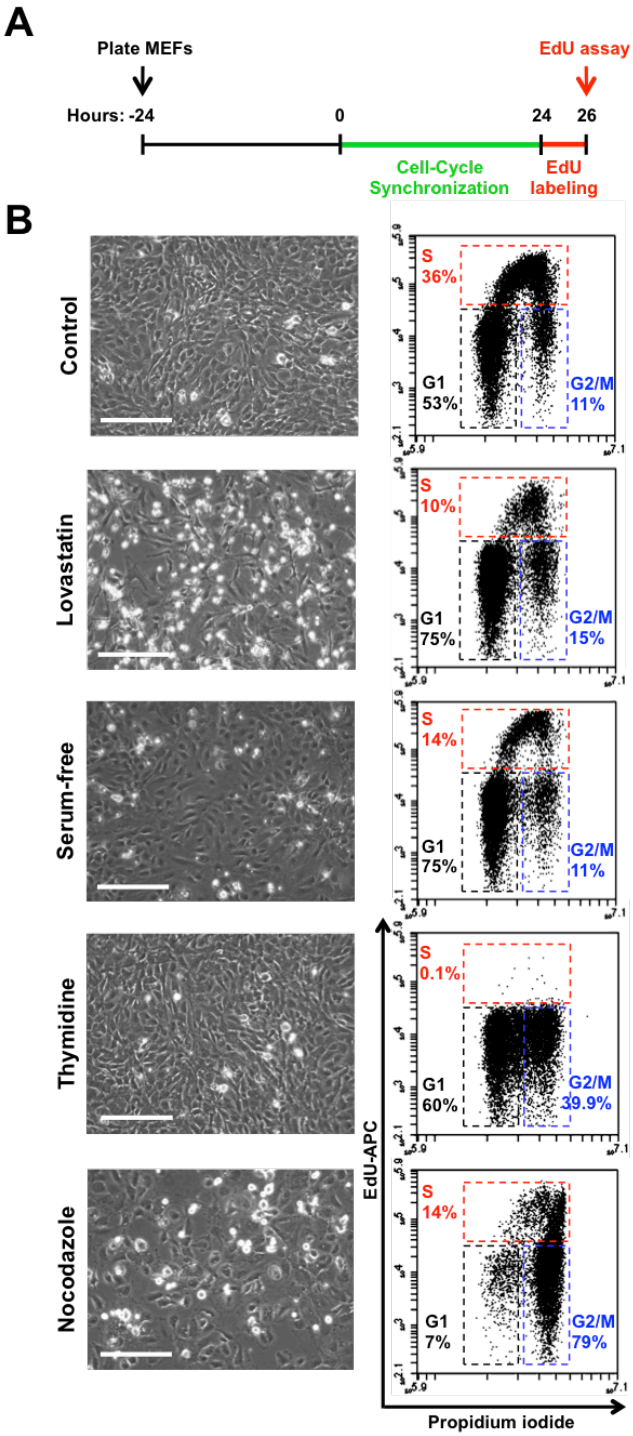

Figure 5. Cell-cycle synchronization of MEFs. A) Experimental schema of cell-cycle synchronization and EdU assay. **B**) Representative pictures (left) and FACS plots (Right) of MEFs without (Control) or with a 24-hour incubation of lovastatin (G1), serum-free media (G0/G1), thymidine (G1/S), and nocodazole (G2/M). Scale bars indicate 100µm.

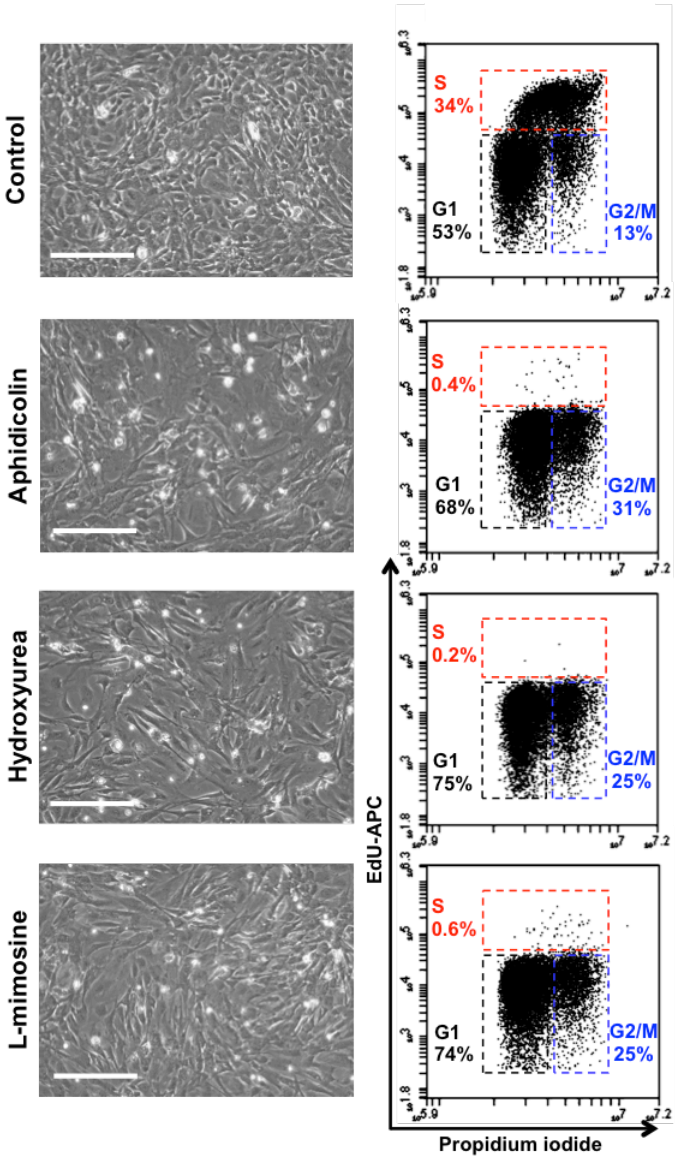

Figure 6. S-phase synchronization of MEFs. Representative pictures (left) and FACS plots (Right) of MEFs without (control) or with a 24-hour incubation of aphidicolin, hydroxyurea, or L-mimosine synchronization. Scale bars indicate 100μm.

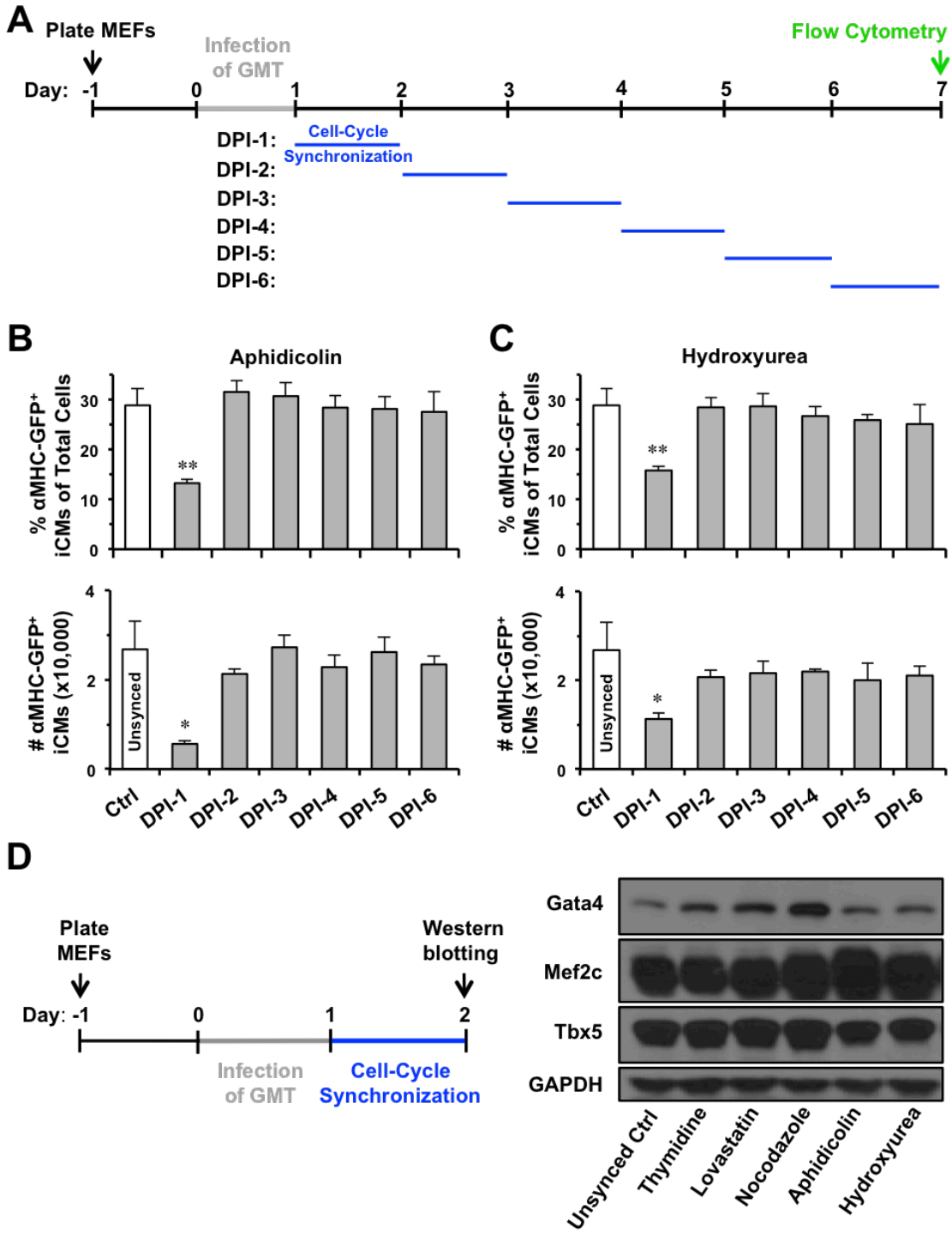

Figure 7 DPI-1 is a critical time window for regulating iCM-reprogramming. A) Schema of experimental design. **B-C**) The effect of S-phase synchronization by aphidicolin **(B)** or hydroxyurea **(C)** from DPI-1 to DPI-6 on the percentage and absolute number of GMT-iCMs. *p<0.05; **p<0.01 vs. control. **D**) Protein expressions of Gata4, Mef2c, and Tbx5 in MEFs were not inhibited by any treatments of cell-cycle synchronization.

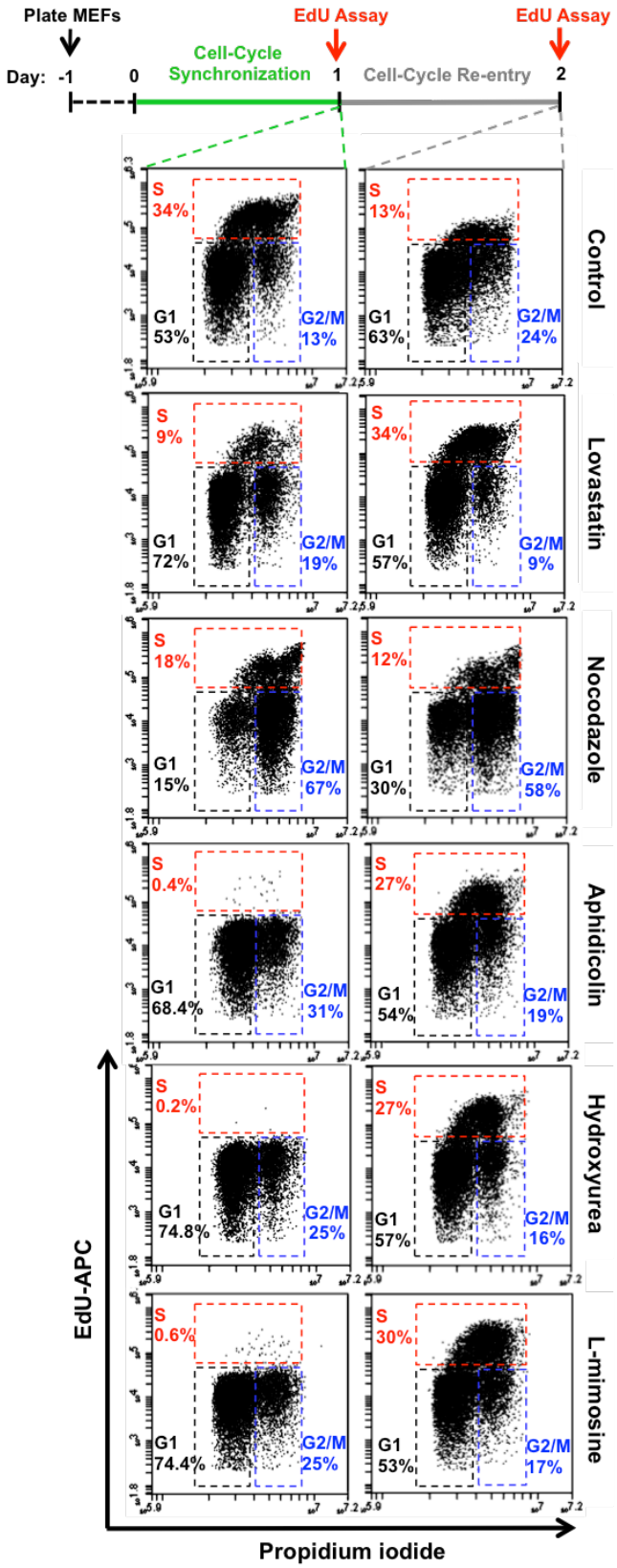

Figure 8. Synchronized MEFs can reenter cell cycle within 24 hrs. FACS plots show that un-reprogrammed MEFs were synchronized into different cell-cycle phases by relevant treatments (left) and reentered cell cycle 24 hours after releasing from synchronization (Right).

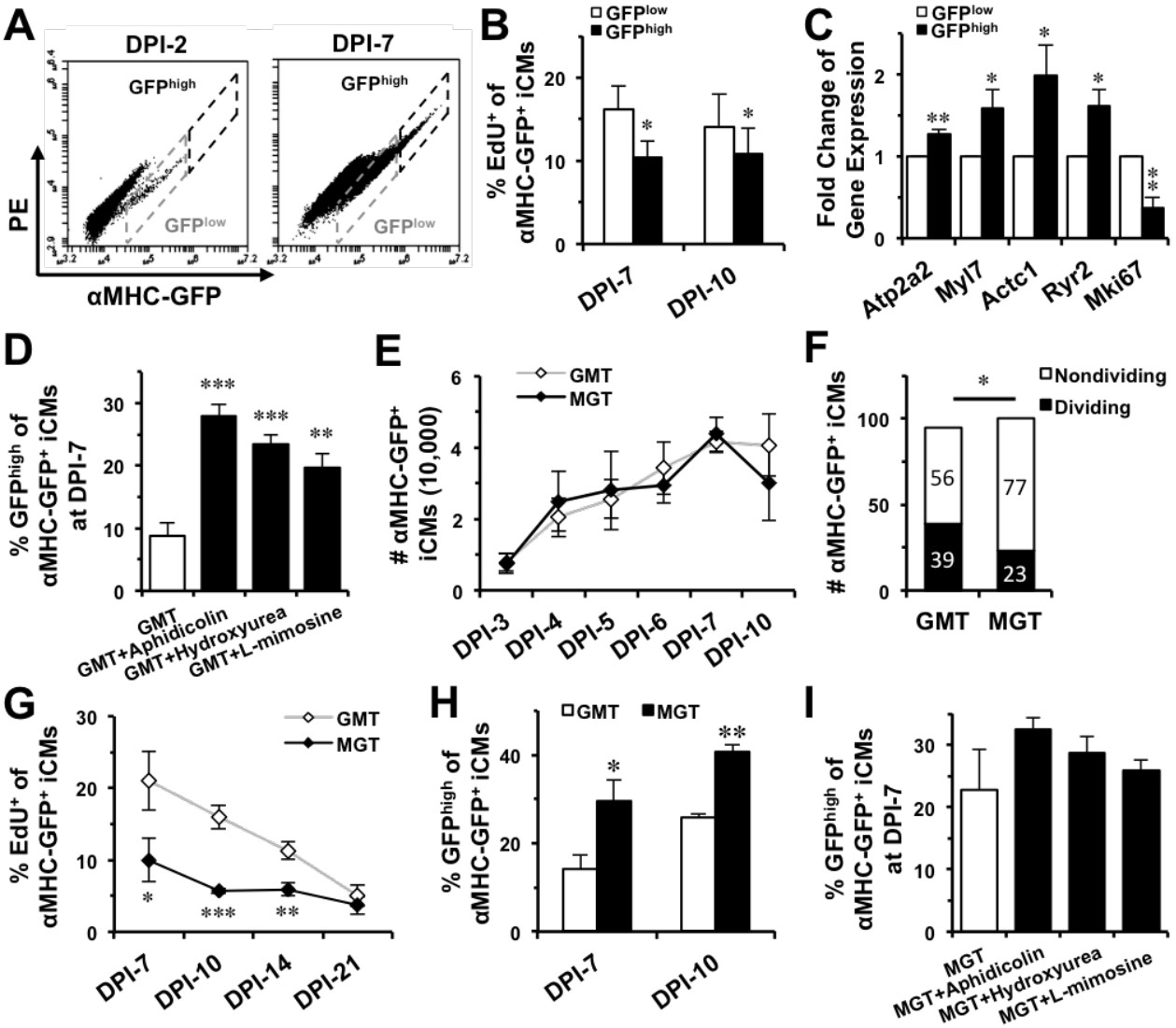

Figure 9. S-phase synchronization or a polycistronic construct (MGT) accelerates the early progression of reprogramming and increases the yield of GFP^{high} iCMs. A) Reprogrammed iCMs were classified into GFP^{low} and GFP^{high} populations. **B)** Significantly less GFP^{high} iCMs were stained positive for EdU than GFP^{low} cells at DPI-7 (n=3) and DPI-10 (n=6). **C)** Comparisons of gene expression in GFP^{low} and GFP^{high} iCMs (n=6). **D)** S-phase synchronization at DPI-1 significantly increased GFP^{high} cells of GMT-iCMs (n=11). **E)** A similar number of αMHC-GFP^{+} iCMs (n=3) were reprogrammed by polycistronic MGT or monocistronic GMT. **F)** Time-lapse recordings revealed significantly less dividing cells among MGT-iCMs than that among GMT-iCMs. **G)** EdU assays showed that MGT-iCMs exited cell cycle earlier than GMT-iCMs (n=3). **H)** MGT-reprogramming yielded more GFP^{high} iCMs than GMT-reprogramming at DPI-7 (n=7) and DPI-10 (n=3). **I)** S-phase synchronization at DPI-1 had no significant improvement on MGT-reprogramming (n=4). *p<0.05, **p<0.01 vs. control.

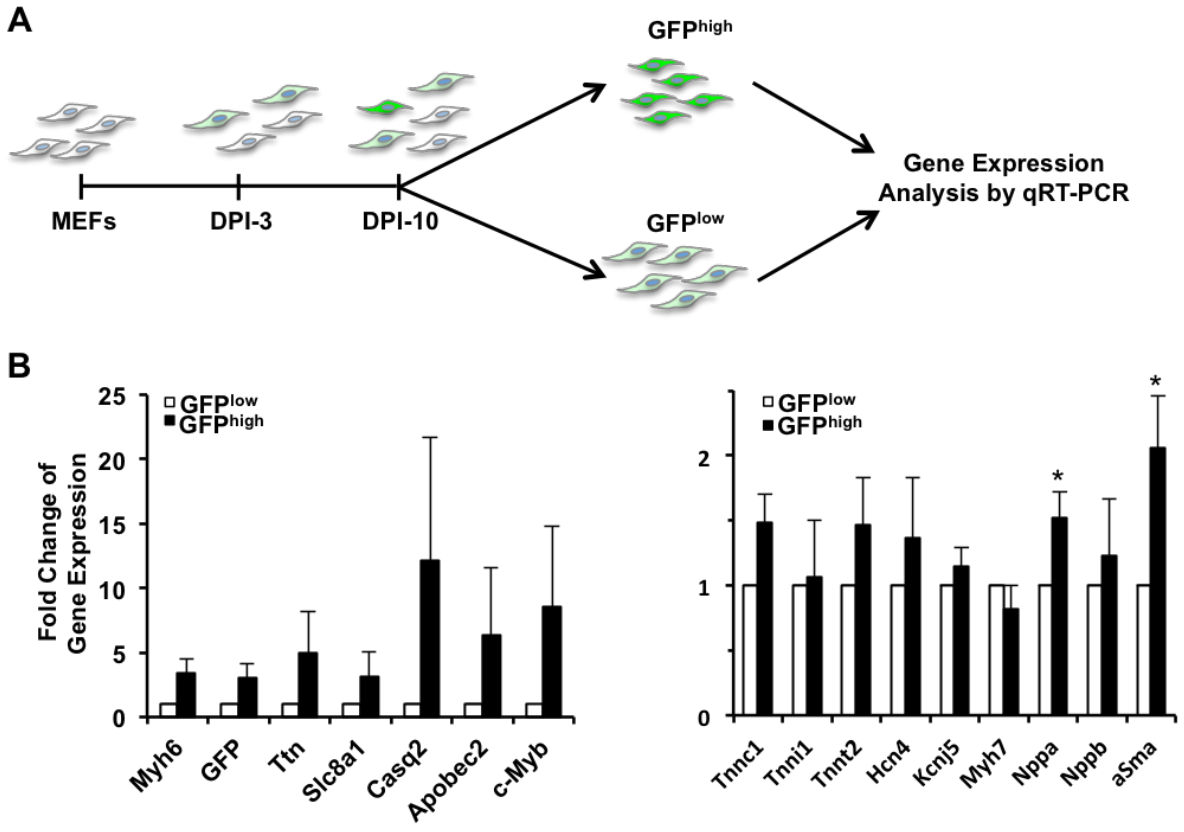

Figure 10. Cardiac genes were expressed higher in GFP^{high} iCMs than that in GFP^{low} cells. A) Schema of experimental design. **B**) qRT-PCR analysis of cardiac genes in GFP^{low} and GFP^{high} iCMs (n=4). *p<0.05 vs. GFP^{low}.

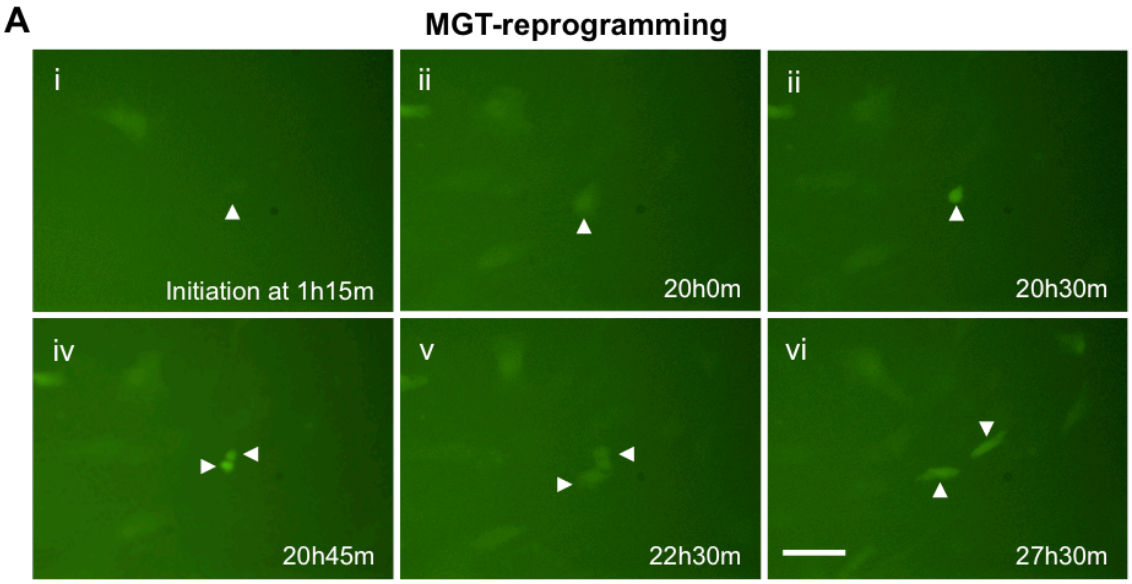

B

αMHC-GFP+ MGT-iCMs	Primary	Doubling	Cell Death	Yield
Nondividing	77		2	75
Dividing	23	+23	4	42
Total	100	23	6	117
	123		123	

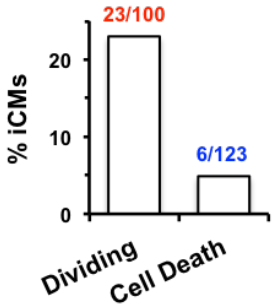

Figure 11. MGT-iCMs go through cell division at the early stage of reprogramming. A) Representative images of time-lapse recording showing that one MGT-iCM (arrowhead) divided into two daughter iCMs. Scale bar indicates 50μm. **B**) A table summarizing the time-lapse result of MGT-reprogrammed αMHC-GFP^{+} iCMs. Bar graph shows the percentage of dividing MGT-reprogrammed iCMs and cells that underwent cell death.

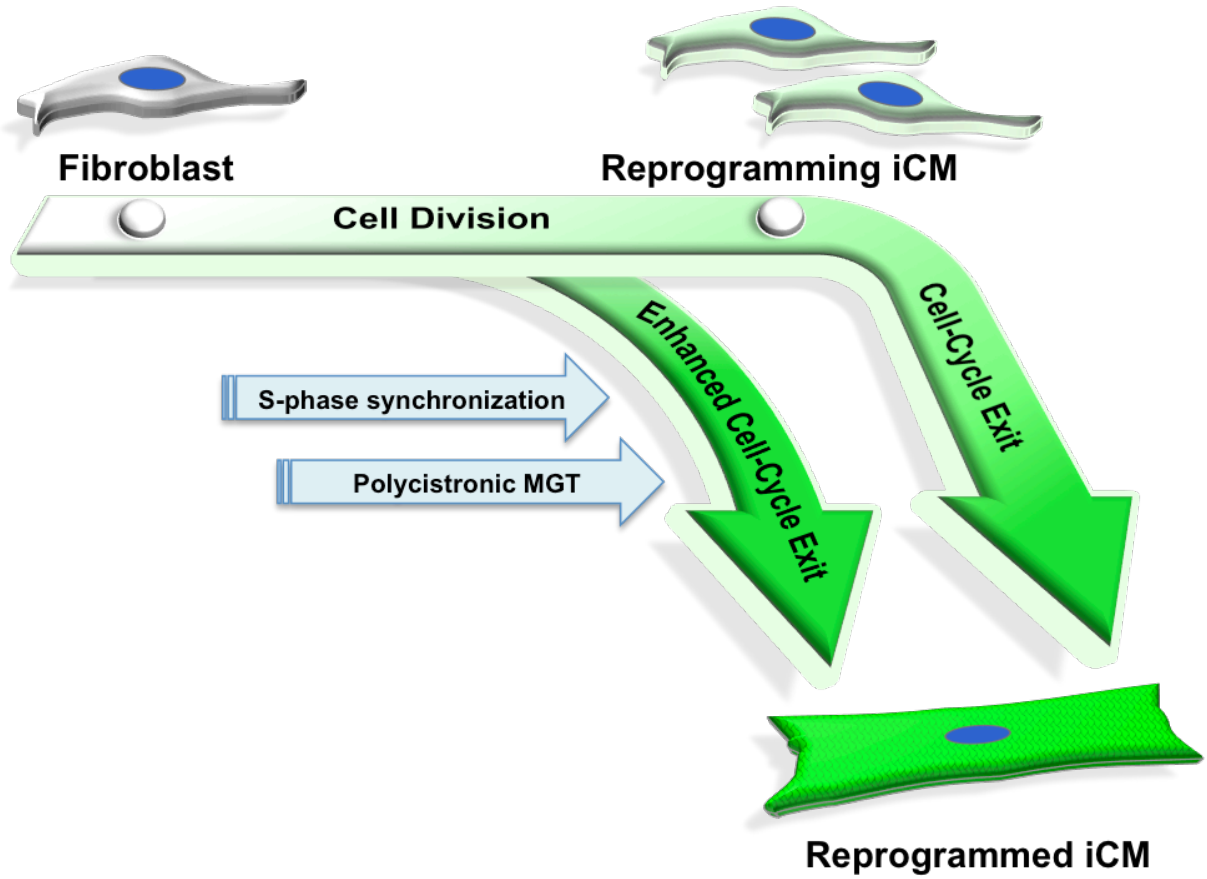

Figure 12. Proposed mechanism of reprogramming acceleration with enhanced cell-cycle exit

Table 1. qRT-PCR primers for gene expression analysis of iCMs

Gene	Primer sets		Product size (bp)
Atp2a2	F R	5'- TCTACGTGGAACCTTTGCCG -3' 5'- GCTGCACACACTCTTTACCG -3'	162
Myl7	F R	5'- GGTCCCATCAACTTCACCGT -3' 5'- AAGGCACTCAGGATGGCTTC -3'	86
Actc1	F R	5'- TGCCATGTATGTCGCCATCC -3' 5'- CACCATCGCCAGAATCCAGA -3'	86
Ryr2	F R	5'- ACGGCGACCATCCACAAAG -3' 5'- AAAGTCTGTTGCCAAATCCTTCT -3'	67
Myh6	F R	5'- GCCCAGTACCTCCGAAAGTC -3' 5'- GCCTTAACATACTCCTCCTTGTC -3'	110
GFP	F R	5'- GGACGACGGCAACTACAAGA -3' 5'- AAGTCGATGCCCTTCAGCTC -3'	87
Ttn	F R	5'- CCGATGTTTACGCAGCCGTTA -3' 5'- TCAAAGGTTGCGGTACTACCC -3'	62
Slc8a1	F R	5'- CTTCCCTGTTTGTGCTCCTGT -3' 5'- AGAAGCCCTTTATGTGGCAGTA -3'	78
Casq2	F R	5'- GCCCAACGTCATCCCTAACA -3' 5'- CCCATTCAAGTCGTCTTCCCA -3'	133
Apobec2	F R	5'- GATCTTCCGCCCTTCGAGATT -3' 5'- TCTGTACTTCGACCACATAGCA -3'	130
c-Myb	F R	5'- AGACCCCGACACAGCATCTA -3' 5'- CAGCAGCCCATCGTAGTCAT -3'	81
Tnnc-1	F R	5'- GGAGCTGTCGGATCTCTTCC -3' 5'- GGCCATCGTTGTTCTTGTCAC -3'	155
Tnni-1	F R	5'- ACCATGCCGGAAGTTGAGAG -3' 5'- GAATGCGCTCCGAGAGGTAA -3'	151
Tnnt-2	F R	5'- ACAGAGGAGGCCAACGTAGA -3' 5'- AAGTTGGGCATGAAGAGCCT -3'	113
Hcn4	F R	5'- ACTCCTGGGGGAAGCAGTAT -3' 5'- GCCGATGAACATGGCATAGC -3'	158
Kcnj5	F R	5'- ATACTCCTTCTGGTGCAGGC -3' 5'- GCTCTCTTCTTTGGCTGGCT -3'	95
Myh7	F R	5'- ACTGTCAACACTAAGAGGGTCA -3' 5'- TTGGATGATTTGATCTTCCAGGG -3'	114
Nppa	F R	5'- CCCTCGGAGCCTACGAAGAT -3' 5'- TGTTGCAGCCTAGTCCACTC -3'	80
Nppb	F R	5'- GATCCGTCAGTCGTTTGGGC -3' 5'- AAAGAGACCCAGGCAGAGTCA -3'	98
MKi67	F R	5'- ATCATTGACCGCTCCTTTAGGT -3' 5'- GCTCGCCTTGATGGTTCCT -3'	104
aSMA	F R	5'- ATCACCAACTGGGACGACAT -3' 5'- CATACATGGCTGGGACATTG -3'	175
Gapdh	F R	5'- AGGTCGGTGTGAACGGATTTG -3' 5'- TGTAGACCATGTAGTTGAGGTCA -3'	123

2.5. DISCUSSION

In this study, we focused on understanding the early progression of iCM-reprogramming and found that iCMs did go through cell division at the early stage of reprogramming and ultimately exited cell cycle during the process of reprogramming. Importantly, we found that S-phase synchronization at the critical initiation time of reprogramming (DPI-1) facilitated the early progression of GMT-reprogramming and yielded more GFP^{high} iCMs through a mechanism of enhancing cell-cycle exit.

Cell cycle includes two critical phases—a synthesis phase (S-phase) of accurate DNA duplication and a mitosis phase of chromosome segregation—which are preceded by two gap phases, G1- and G2-phase respectively. Although epigenetic status at S and G2/M phases suppresses global RNA transcription and protein synthesis, with the exception of histone proteins (**Bou Kheir et al., 2010**), our time-lapse recordings revealed that the activation of αMHC-GFP was majorly initiated at late G1 and S-phases and iCM-reprogramming is processed and continued through more than one cell-cycle. Many reprogrammed iCMs did go through cell division soon after αMHC-GFP activation. Very recently, single-cell transcriptomics of reprogrammed iCMs reconstructs a path of cell-fate conversion from fibroblast to iCMs and disclosed a population of early-stage reprogrammed iCMs that underwent cell division (**Liu et al., 2017**). Furthermore, consistently with previous studies (**Addis et al., 2013; Yamakawa et al., 2015; Zhou et al., 2017b**), we also found that reprogrammed iCMs exited cell cycle at a later stage of reprogramming, and S-phase synchronization at DPI-1 facilitated cell-cycle exit in GMT-iCMs and yielded fewer reprogrammed iCMs.

Interestingly, the facilitated cell-cycle exit by S-phase synchronization at DPI-1 was accompanied with an improved progression of GMT-reprogramming and yielded significantly more GFP^{high} iCMs, which achieved a more advanced reprogramming than GFP^{low} cells. This might be due to that cell-cycle exit prevents a dilution of GMT expression in individual iCMs and subsequently induce high cardiac gene

expression and better reprogramming. It is also true in iCM-reprogramming of polycistronic MGT (**Wang et al., 2015**), which accelerated cell-cycle exit and yielded more GFP^{high} iCMs. Because of this accelerated progression of MGT-reprogramming, S-phase synchronization failed to further increase the GFP^{high} portion in MGT-iCMs. It has been shown that active cell-cycle status and maturity have negative correlation in iCMs (**Zhou et al., 2017b**). On the other hand, it has been observed that iCM-reprogramming was significantly suppressed in an immortalized cardiac fibroblast line that will never exit cell cycle (**Liu et al., 2017**), indicating the importance of cell-cycle exit in iCM-reprogramming. Noticeably, our time-lapse recordings also found that some iCMs reprogrammed by either GMT or MGT underwent cell death, possibly apoptosis, which could explain why inhibitors of ROCK signaling increased the yield of reprogrammed iCMs (**Zhao et al., 2015**).

In summary, our study provides direct evidence that iCMs actually go through cell division at an early reprogramming stage and exit cell cycle along the process of reprogramming. Importantly, our studies suggest that cell-cycle exit is one critical event or an indicator of the transition into a more advanced reprogramming. Enhanced cell-cycle exit by S-phase synchronization promotes the early progression of iCM-reprogramming. Our study provides a mechanistic understanding of iCM-reprogramming, which will help us to translate this nascent reprogramming technique into a therapeutic paradigm in the future.

2.6. FUTURE DIRECTIONS

In this study, we showed that S-phase synchronization have particular effect on maturation of iCMs during reprogramming process through enhancing cell cycle exit. There are some major points to be addressed in the future studies.

First, we showed that iCM induction was achieved majorly at late-G1 and S phases, possibly through increased accession of reprogramming factors to cardiac gene promoters. Extended S-phase by cell cycle synchronization might impose a special epigenetic status, which in turn might allow increased transcription of cardiac genes. These suggest that iCM induction might require at least one G1/S transition during initiation of reprogramming. Therefore, it needs to be validated through more vigorous experiments whether iCM reprogramming essentially requires S-phase epigenetics.

Second point, which needs to be clarified, is the mechanism imposed by S-phase on cell cycle exit. It is still unknown why S-phase particularly inducing cell cycle exit in iCMs during reprogramming process while not in the plain fibroblasts (**Figure 8**). However, the findings by **Barr et al** (**2017**) supports that S or G2/M phase arrest in iCMs by the drugs might induce cell cycle exit in the subsequent cell cycle phases possibly through DNA damage response mechanisms. Regardless of this conclusion, mechanism of action for facilitated cell cycle exit in iCMs needs to be more extensively examined in future studies.

Another important point is how important the cell-cycle exit is for iCMs. S-phase and use of MGT polycistronic construct improved maturity of iCMs and enhanced cell-cycle exit, meaning that cell-cycle exit and iCM maturity have positive correlation. The more the chance of cell cycle exit, the better the maturity of iCMs. Cell cycle exit in native cardiomyocytes has been an interesting topic so far, however, mechanism of cell cycle exit has not been much understood. Therefore, iCMs generated by S-phase could be used as a model to understand what really derives cell cycle exit in cardiomyocytes or why it helps

maturity of cardiomyocytes. There is a possibility that cardiomyocytes or iCMs exit cell cycle to prevent DNA damage so that they can preserve their genomic stability. It might be also possible that telomere length is different in reprogrammed iCMs or cardiomyocytes; therefore, they might be more prone to DNA damages during active cell cycle progression. However, all these are speculations and need to be addressed in future studies.

Last but not least, GFP^{high} iCMs were used as a measure of reprogramming quality in our study, however, functional aspects of GFP^{high} cells, e.g. beating or calcium flux, have not been studied. Therefore, it needs to be further validated whether those cells are functionally more mature as well as their maturity in expression of cardiac genes. On the other hand, varying intensities of GFP might be a good indicator for reprogramming degree of iCMs and could be used for evaluation of reprogramming quality. Therefore, single cell quantitative RT-PCR analysis of cells with varying GFP intensities might verify their degree of reprogramming and should be addressed in the future studies. Evaluation by GFP^{high} iCM population might allow us to speed up our quality assessment when comparing two or more experimental groups. This could be a helpful way to use in screening novel drugs, RNAs, or compounds which improve quality and maturity but not the number or percentage of iCMs. Also, this strategy might be applicable in reprogramming of other cell types, which uses fluorescent reporters as similar to αMHC-GFP.

2.7. REFERENCES

1. Addis, R.C., Ifkovits, J.L., Pinto, F., Kellam, L.D., Esteso, P., Rentschler, S., Christoforou, N., Epstein, J.A., and Gearhart, J.D. (2013). Optimization of direct fibroblast reprogramming to cardiomyocytes using calcium activity as a functional measure of success. J. Mol. Cell. Cardiol. *60*, 97–106. DOI: 10.1016/j.yjmcc.2013.04.004
2. Barr, A., Cooper, S., Heldt, F., Butera, F., Stoy, H., Mansfeld, J., Novák, B., and Bakal, C. (2017). DNA damage during S-phase mediates the proliferation-quiescence decision in the subsequent G1 via p21 expression. Nat Commun *8*, 14728.
3. Bou Kheir, T., and Lund, A.H. (2010). Epigenetic dynamics across the cell cycle. Essays Biochem. *48*, 107–20. DOI: 10.1042/bse0480107
4. Buganim, Y., Faddah, D., and Jaenisch, R. (2013). Mechanisms and models of somatic cell reprogramming. Nat Rev Genet *14*, 427–439. DOI: 10.1038/nrg3473
5. Chen, M., Huang, J., Yang, X., Liu, B., Zhang, W., Huang, L., Deng, F., Ma, J., Bai, Y., Lu, R., et al. (2012). Serum starvation induced cell cycle synchronization facilitates human somatic cells reprogramming. PLoS ONE *7*, e28203. DOI: 10.1371/journal.pone.0028203
6. Fu, J.D., Stone, N.R., Liu, L., Spencer, C.I., Qian, L., Hayashi, Y., Delgado-Olguin, P., Ding, S., Bruneau, B.G., and Srivastava, D. (2013). Direct reprogramming of human fibroblasts toward a cardiomyocyte-like state. Stem Cell Reports *1*, 235–47. DOI: 10.1016/j.stemcr.2013.07.005
7. Ieda, M., Fu, J.D., Delgado-Olguin, P., Vedantham, V., Hayashi, Y., Bruneau, B.G., and Srivastava, D. (2010). Direct reprogramming of fibroblasts into functional cardiomyocytes by defined factors. Cell *142*, 375–86. DOI: 10.1016/j.cell.2010.07.002
8. Ifkovits, J.L., Addis, R.C., Epstein, J.A., and Gearhart, J.D. (2014). Inhibition of TGFβ signaling increases direct conversion of fibroblasts to induced cardiomyocytes. PLoS ONE *9*, e89678. DOI: 10.1371/journal.pone.0089678

9. Jayawardena, T.M., Finch, E.A., Zhang, L., Zhang, H., Hodgkinson, C.P., Pratt, R.E., Rosenberg, P.B., Mirotsou, M., and Dzau, V.J. (2015). MicroRNA induced cardiac reprogramming in vivo: evidence for mature cardiac myocytes and improved cardiac function. Circ. Res. *116*, 418–24. DOI: 10.1161/CIRCRESAHA.116.304510

10. Jiang, H., Xu, Z., Zhong, P., Ren, Y., Liang, G., Schilling, H., Hu, Z., Zhang, Y., Wang, X., Chen, S., et al. (2015). Cell cycle and p53 gate the direct conversion of human fibroblasts to dopaminergic neurons. Nat Commun *6*, 10100. DOI: 10.1038/ncomms10100

11. Liu, Z., Wang, L., Welch, J.D., Ma, H., Zhou, Y., Vaseghi, H.R., Yu, S., Wall, J.B., Alimohamadi, S., Zheng, M., et al. (2017). Single-cell transcriptomics reconstructs fate conversion from fibroblast to cardiomyocyte. Nature. Epublished. DOI: 10.1038/nature24454

12. Ma, H.T., and Poon, R.Y. (2011). Synchronization of HeLa cells. Methods Mol. Biol. *761*, 151–61. DOI: 10.1007/978-1-61779-182-6_10

13. Mohamed, T.M., Stone, N.R., Berry, E.C., Radzinsky, E., Huang, Y., Pratt, K., Ang, Y.-S.S., Yu, P., Wang, H., Tang, S., et al. (2017). Chemical Enhancement of In Vitro and In Vivo Direct Cardiac Reprogramming. Circulation *135*, 978–995. DOI: 10.1161/CIRCULATIONAHA.116.024692

14. Muraoka, N., Yamakawa, H., Miyamoto, K., Sadahiro, T., Umei, T., Isomi, M., Nakashima, H., Akiyama, M., Wada, R., Inagawa, K., et al. (2014). MiR-133 promotes cardiac reprogramming by directly repressing Snai1 and silencing fibroblast signatures. EMBO J. *33*, 1565–81. DOI: 10.15252/embj.201387605

15. Nam, Y.J., Song, K., Luo, X., Daniel, E., Lambeth, K., West, K., Hill, J.A., DiMaio, J.M., Baker, L.A., Bassel-Duby, R., et al. (2013). Reprogramming of human fibroblasts toward a cardiac fate. Proc. Natl. Acad. Sci. U.S.A. *110*, 5588–93. DOI: 10.1073/pnas.1301019110

16. Rosner, M., Schipany, K., and Hengstschläger, M. (2013). Merging high-quality biochemical fractionation with a refined flow cytometry approach to monitor nucleocytoplasmic protein

expression throughout the unperturbed mammalian cell cycle. Nat Protoc *8*, 602–26. DOI: 10.1038/nprot.2013.011

17. Song, K., Nam, Y.-J.J., Luo, X., Qi, X., Tan, W., Huang, G.N., Acharya, A., Smith, C.L., Tallquist, M.D., Neilson, E.G., et al. (2012). Heart repair by reprogramming non-myocytes with cardiac transcription factors. Nature *485*, 599–604. DOI: 10.1038/nature11139

18. Van Berlo JH, Molkentin JD. An emerging consensus on cardiac regeneration. *Nat. Med.* 2014; 20:1386–93. doi: 10.1038/nm.3764.

19. Yamakawa, H., Muraoka, N., Miyamoto, K., Sadahiro, T., Isomi, M., Haginiwa, S., Kojima, H., Umei, T., Akiyama, M., Kuishi, Y., et al. (2015). Fibroblast Growth Factors and Vascular Endothelial Growth Factor Promote Cardiac Reprogramming under Defined Conditions. Stem Cell Reports *5*, 1128–42. DOI: 10.1016/j.stemcr.2015.10.019

20. Zhao, Y., Londono, P., Cao, Y., Sharpe, E.J., Proenza, C., O'Rourke, R., Jones, K.L., Jeong, M.Y., Walker, L.A., Buttrick, P.M., et al. (2015). High-efficiency reprogramming of fibroblasts into cardiomyocytes requires suppression of pro-fibrotic signalling. Nat Commun *6*, 8243. DOI: 10.1038/ncomms9243.

21. Zhou, H., Dickson, M.E., Kim, M.S., Bassel-Duby, R., and Olson, E.N. (2015). Akt1/protein kinase B enhances transcriptional reprogramming of fibroblasts to functional cardiomyocytes. Proc. Natl. Acad. Sci. U.S.A.*112*, 11864–9. DOI: 10.1073/pnas.1516237112.

22. Zhou, H., Morales, M.G., Hashimoto, H., Dickson, M.E., Song, K., Ye, W., Kim, M.S., Niederstrasser, H., Wang, Z., Chen, B., et al. (2017a). ZNF281 enhances cardiac reprogramming by modulating cardiac and inflammatory gene expression. Genes Dev. *31*, 1770–1783.

23. Zhou, Y., Wang, L., Vaseghi, H.R., Liu, Z., Lu, R., Alimohamadi, S., Yin, C., Fu, J.D., Wang, G.G., Liu, J., et al. (2016). Bmi1 Is a Key Epigenetic Barrier to Direct Cardiac Reprogramming. Cell Stem Cell *18*, 382–95. DOI: 10.1016/j.stem.2016.02.003.

24. Zhou, Y., Wang, L., Liu, Z., Alimohamadi, S., Yin, C., Liu, J., and Qian, L. (2017b). Comparative Gene Expression Analyses Reveal Distinct Molecular Signatures between

Differentially Reprogrammed Cardiomyocytes. Cell Reports *20*, 3014–3024. DOI: 10.1016/j.celrep.2017.09.005

25. Wada, R., Muraoka, N., Inagawa, K., Yamakawa, H., Miyamoto, K., Sadahiro, T., Umei, T., Kaneda, R., Suzuki, T., Kamiya, K., et al. (2013). Induction of human cardiomyocyte-like cells from fibroblasts by defined factors. Proc. Natl. Acad. Sci. U.S.A. *110*, 12667–72. DOI: 10.1073/pnas.1304053110.

26. Wang L., Liu Z., Yin C., Asfour H., Chen O., Li Y., Bursac N., Liu J., and Qian L. (2015). Stoichiometry of Gata4, Mef2c, and Tbx5 Influences the Efficiency and Quality of Induced Cardiac Myocyte Reprogramming. Circulation Research *116*, 237–244. DOI: 10.1161/CIRCRESAHA.116.305547.

27. Weider, R. (1999). Selection of Methods for Measuring Proliferation. In Cell Growth, Differentiation, and Senescence: A Practical Approach, G.P. Studzinski, ed. (Oxford: Oxford University Press) pp. 1-32.

28. Qian L., Huang Y., Spencer C.I., Foley A., Vedantham V., Liu L., Conway S.J., Fu J.D., Srivastava D. (2012). In vivo reprogramming of murine cardiac fibroblasts into induced cardiomyocytes. Nature 485, 593–598. DOI: 10.1038/nature11044.